ADVANCED MATERIALS TECHNOLOGIES
www.advmattechnol.de

Fundamentals, Materials, and Applications for Daytime Radiative Cooling

Zizhong Li, Qiyuan Chen, Yan Song, Bin Zhu, and Jia Zhu**

Daytime radiative cooling is emerging as a passive and environmentally friendly cooling strategy, compared to traditional cooling methods that consume a vast amount of energy with a significant carbon footprint. To achieve the best cooling performance, materials tailored for daytime radiative cooling need to generate high emission in the atmospheric transmission window (8–13 µm) for radiating heat out directly to the universe and simultaneously reflect the entire solar radiation to minimize the thermal load. Recently, daytime subambient radiative cooling has been demonstrated through a range of novel material strategies. Herein, the fundamental principles for nighttime and daytime radiative cooling are summarized, and different designs of materials and structures suitable for substantial cooling performances are highlighted, together with various real-world applications including building, water cooling, and clothing. Several possible pathways of daytime radiative cooling for further development are also outlined. It is anticipated that this review will provide an overall picture of recent progress and inspire more efforts into the fundamental understanding and practical applications of daytime radiative cooling.

1. Introduction

Cooling plays a vital role in human life. Unfortunately, traditional cooling methods, such as air conditioner (AC), usually consume a vast amount of energy with a significant carbon footprint. Therefore, it would be ideal to develop energy-saving and environment-friendly cooling strategies. An appealing technique is radiative cooling, which employs the universe (typical temperature is about 3 K) as a natural heat sink to absorb heat that generated from the earth (300 K) through thermal radiation. It demands no extra energy input and only uses a device or material to radiate heat to the outer space through a transparency window in the atmosphere between 8 and 13 µm.

In the last century, several groups proposed the concept of radiative cooling and developed nighttime radiative cooling by designing various materials with high emissivity in the wavelength of 8–13 µm. Achieving daytime radiative cooling to a temperature below ambient under sunlight is difficult because the incoming solar radiation is intense and can easily counteract the outgoing thermal radiation to outer space.

In 2014, Fan's group first experimentally achieved the daytime radiative cooling below the ambient air temperature under direct sunlight using an integrated photonic solar reflector and thermal emitter.[1] Afterward, other material designs, including metamaterials[2] and porous polymers,[3] have been proposed to achieve daytime radiative cooling. The rapidly developed technique also brings a wide range of practical applications in building, water cooling, air cooling, and clothing.

In this review, we systematically discuss the fundamentals for radiative cooling, summarize recent advancements in daytime radiative cooling, and introduce its real-world applications (**Figure 1**). Meanwhile, we also propose scopes for further developments. Because of its nonenergy-consuming characteristic, we believe passive daytime radiative cooling will be a promising area for energy-saving cooling methods and expect more efforts in the practical applications.

2. Fundamentals and Principles

2.1. Atmospheric Transparency Window

Radiative cooling (**Figure 2**a) below ambient air temperature has already been achieved by taking advantage of the atmospheric transparency window.[4] The atmosphere is transparent for radiation in the wavelength range between 8 and 13 µm (Figure 2b), which also overlaps the spectral realm of peak thermal radiation at typical ambient temperature. Therefore, terrestrial emitters can effectively exchange energy with the largest heat sink, the universe, via thermal radiation through the atmospheric transparency window. To better understand this cooling effect, we need to investigate the heat flow components of the emitter.

2.2. Heat Flow of Radiative Cooling

Consider an emitter at temperature T with a spectral and angular emissivity $\varepsilon(\lambda, \theta)$. The emitter is exposed to the sky in direct sunlight, then the net cooling power P_{cool} is given by[8]

Z. Li, Q. Chen, Dr. Y. Song, Dr. B. Zhu, Prof. J. Zhu
National Laboratory of Solid State Microstructures
College of Engineering and Applied Sciences
Jiangsu Key Laboratory of Artificial Functional Materials
Nanjing University
Nanjing 210093, P. R. China
E-mail: binzhu@nju.edu.cn; jiazhu@nju.edu.cn
The ORCID identification number(s) for the author(s) of this article can be found under https://doi.org/10.1002/admt.201901007.

DOI: 10.1002/admt.201901007

© 2020 WILEY-VCH Verlag GmbH & Co. KGaA, Weinheim

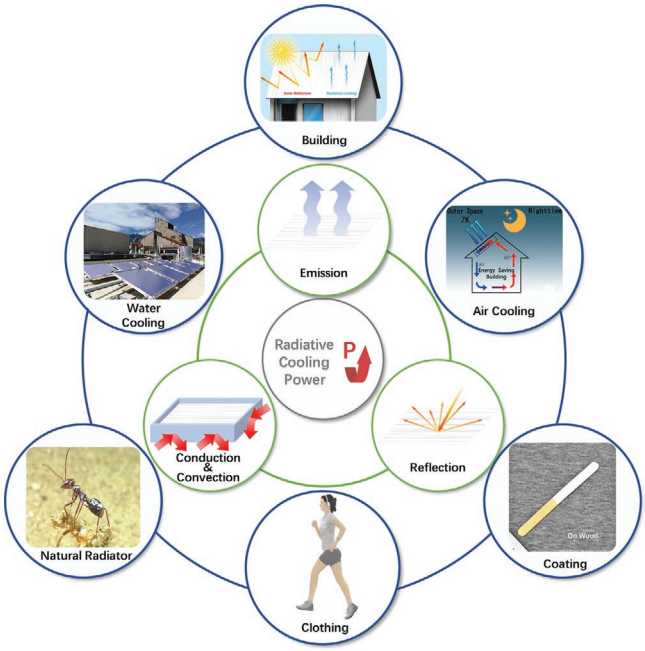

Figure 1. Outline of daytime radiative cooling. Inner (gray) layer: Demand for daytime radiative cooling. Middle (green) layer: Materials and devices design criterion. Outer (blue) layer: Applications of daytime radiative cooling. Building (Reproduced with permission.[28] Copyright 2019, The American Association for the Advancement of Science), air cooling (Reproduced with permission.[84] Copyright 2019, Elsevier), coating (Reproduced with permission.[3] Copyright 2018, The American Association for the Advancement of Science), clothing (Reproduced with permission.[67] Copyright 2018, John Wiley and Sons), natural radiator (Reproduced with permission.[64] Copyright 2015, The American Association for the Advancement of Science), and water cooling (Reproduced with permission.[34] Copyright 2019, Elsevier).

$$P_{\text{cool}}(T) = P_{\text{rad}}(T) - P_{\text{atm}}(T_{\text{amb}}) - P_{\text{sun}} - P_{\text{cond+conv}} \quad (1)$$

In Equation (1), the power radiated out by the emitter is

$$P_{\text{rad}}(T) = A\int \mathrm{d}\Omega \cos\theta \int_0^\infty \mathrm{d}\lambda I_{\text{BB}}(T,\lambda)\varepsilon(\lambda,\theta) \quad (2)$$

Here, A is the area of the emitter, $I_{\text{BB}}(T,\lambda) = \frac{2hc^2}{\lambda^5}\frac{1}{e^{\frac{hc}{\lambda k_B T}} - 1}$ is the spectral radiance of a blackbody at temperature T, h is Planck's constant, k_B is the Boltzmann constant, c is the speed of light, and λ is the wavelength.

The power absorbed by the emitter from the atmospheric radiation is

$$P_{\text{atm}}(T_{\text{amb}}) = A\int \mathrm{d}\Omega \cos\theta \int_0^\infty \mathrm{d}\lambda\, I_{\text{BB}}(T_{\text{amb}},\lambda)\varepsilon(\lambda,\theta)\varepsilon_{\text{atm}}(\lambda,\theta) \quad (3)$$

The angle-dependent emissivity $\varepsilon_{\text{atm}}(\lambda,\theta)$ is given by $\varepsilon_{\text{atm}}(\lambda,\theta) = 1 - t(\lambda)^{1/\cos\theta}$, where $t(\lambda)$ is the atmospheric transmittance in the zenith direction (Figure 2c) and T_{amb} is the ambient air temperature.[1,6]

The power absorbed by the emitter from solar radiation and diffused sunlight is

$$P_{\text{sun}} = A\int_0^\infty \mathrm{d}\lambda\varepsilon(\lambda,0) I_{\text{AM sw1.5}}(\lambda) + A\int \mathrm{d}\Omega\cos\theta\int_0^\infty \mathrm{d}\lambda I_{\text{solar-diffuse}}(\lambda)\varepsilon(\lambda,\theta) \quad (4)$$

Zizhong Li is an undergraduate student under the direction of Prof. Jia Zhu at Nanjing University. His current research interest is thermoelectric energy conversions.

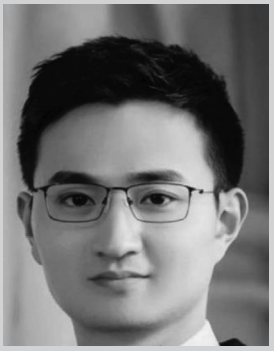

Bin Zhu received his B.S. degree in materials physics from Nanjing University in 2013 and his Ph.D. in materials science and engineering from Nanjing University in 2018. He is currently a research scientist and his research interests include energy storage and solar thermal materials.

Jia Zhu received his B.S. in physics from Nanjing University in China in 2003 and his M.S. and Ph.D. in electrical engineering from Stanford University in 2006 and 2010, respectively. He went on to work as a postdoctoral scholar at the University of California, Berkeley. In 2013, he became a professor in the College of Engineering and Applied Sciences at Nanjing University. He leads a group of researchers working on nanomaterials for energy conversion and storage.

In Equation (5), $I_{\text{AM1.5}}(\lambda)$ is the AM1.5 Global tilt solar illumination with an irradiance of 964 W m^{-2} which is the average solar conditions of the continental US,[8] and $I_{\text{solar-diffuse}}(\lambda)$ is the scattering solar radiation toward the emitter.

The power lost due to heat conduction and convection is[1]

$$P_{\text{cond+conv}}(T, T_{\text{amb}}) = Ah_c(T_{\text{amb}} - T) \quad (5)$$

Here $h_c = h_{\text{cond}} + h_{\text{conv}}$ is the collective nonradiative heat coefficient of the emitter.

Equation (1) represents the heat flow network of the emitter and divides the net cooling power into four components. Among all these four terms, only the power radiated by the

© 2020 WILEY-VCH Verlag GmbH & Co. KGaA, Weinheim

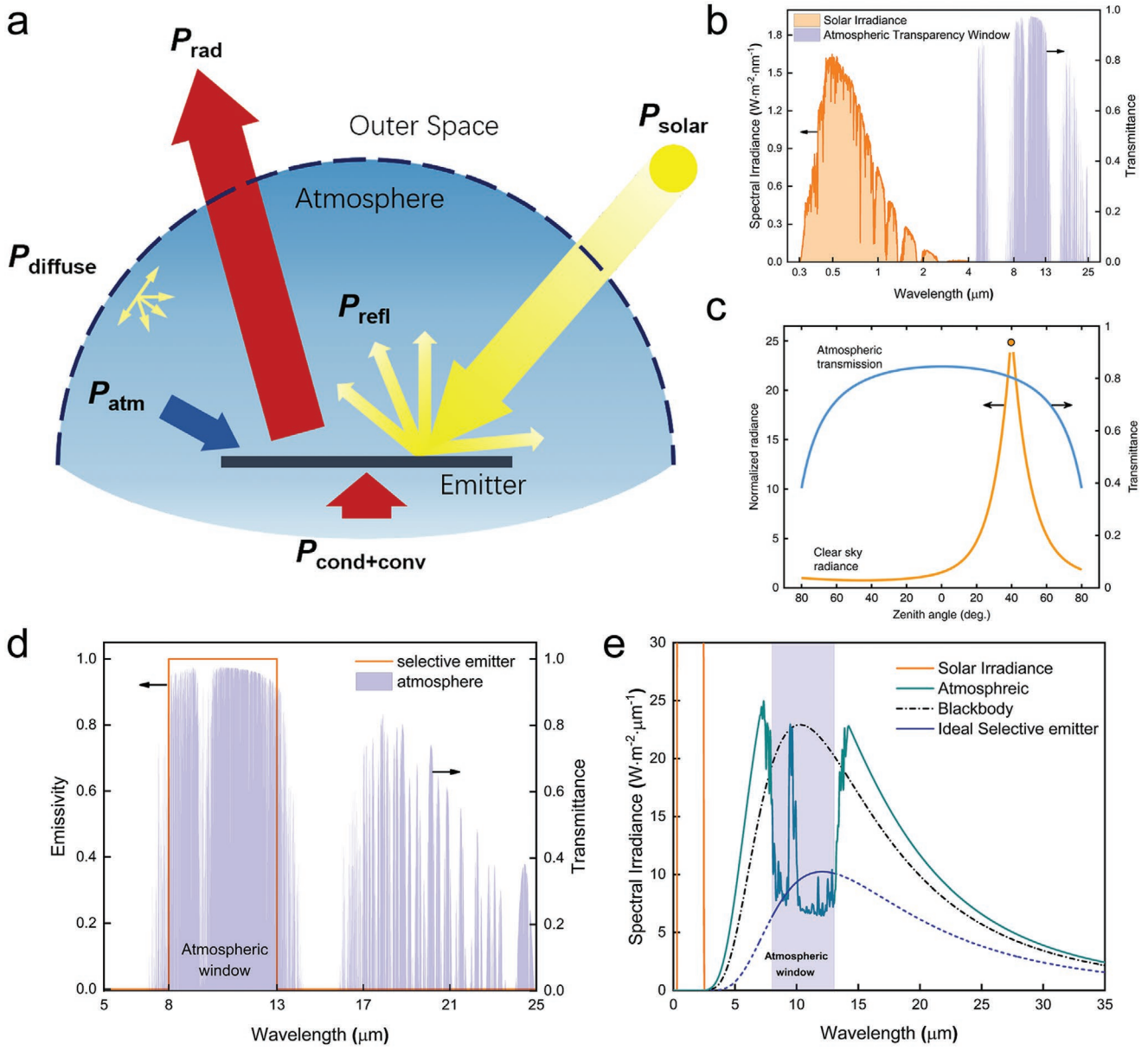

Figure 2. Radiative cooling mechanism. a) Energy flow diagram of the emitter. b) Spectral distribution of solar irradiation and atmospheric transmittance.[5] c) Angular distribution of normalized clear sky radiance in a principal plane that includes the sun (shown for a solar zenith angle of 40°) and atmospheric transmittance. Reproduced with permission.[6] Copyright 2018, Springer Nature. d) Emissivity of an ideal selective emitter matched to 8–13 μm atmosphere window and spectral distribution of atmospheric transmittance. e) The fluxes of blackbody and selective emitter at the equilibrium temperature.[7]

emitter, $P_{rad}(T)$, is outflow, which means the emitter can only dissipate heat through thermal radiation. The emitter becomes a radiative cooling device only if the net power is positive when $T = T_{amb}$, or in another way to say, if reaching thermal equilibrium temperature below ambient.

2.3. Spectral View of Radiative Cooling

The ideal condition for high performance of radiative cooling is when P_{rad} is maximized and P_{sun}, P_{atm}, and $P_{cond+conv}$ minimized. A blackbody radiator has the unit emissivity over the entire spectrum, which indicates that a blackbody emitter can maximize P_{rad}. It seems that blackbody is the best choice for radiative cooling. However, according to Kirchhoff's radiation law, for any specific wavelength, an object with higher emissivity also exhibits higher absorptivity. Blackbody strongly absorbs sunlight and atmospheric radiation, which prevents the device from cooling down under direct sunlight.

Let us consider a simplified scenario. Assuming that the emitter is exposed to the nocturnal sky where we can avoid the solar radiation, and there is no heat loss through conduction and convection, then the total heat exchange of the emitter is composed of two parts: the power emitted out and the absorbed

© 2020 WILEY-VCH Verlag GmbH & Co. KGaA, Weinheim

atmospheric radiation. Since the atmosphere is transparent between 8 and 13 μm while opaque in other wavelengths, we can thus treat the atmosphere spectrum as blackbody spectrum but for a few dips in atmospheric transparency window, as the solid green line depicted (Figure 2e).[7] Consequently, the power of atmosphere radiation is the area under the solid green line, and the power of outward radiation is the area under the black dot-dashed line (Figure 2e), which can be quantified by integrating over the whole spectrum

$$P_{\text{atm}}(T_{\text{amb}}) = C\int_0^{\infty} \mathrm{d}\lambda \varepsilon_{\text{atm}}(\lambda) I_{\text{BB}}(T_{\text{amb}}, \lambda) \tag{6}$$

$$P_{\text{rad}}\left(T_{\text{eq}}^{\text{BB}}\right) = C\int_0^{\infty} \mathrm{d}\lambda I_{\text{BB}}\left(T_{\text{eq}}^{\text{BB}}, \lambda\right) \tag{7}$$

Here T_{amb} is the ambient air temperature, $T_{\text{eq}}^{\text{BB}}$ is the blackbody emitter temperature reached at thermal equilibrium, and C is a constant coefficient. Thermal balance is achieved when $P_{\text{atm}}(T_{\text{amb}}) = P_{\text{rad}}(T_{\text{eq}}^{\text{BB}})$, namely, when the two areas under the lines are equal. We find that the blackbody emitter does reach a steady-state temperature $T_{\text{eq}}^{\text{BB}}$ a few degrees below ambient temperature in this situation, but that is not the lowest temperature an emitter can reach.

Now let us consider the case of an ideal selective radiator, the solid blue line in Figure 2e. If the emitter is an ideal selective radiator with an emittance matched perfectly to the atmospheric transparency window (Figure 2d), then the atmosphere radiation power absorbed in and the power radiated out are

$$P_{\text{atm}}(T_{\text{amb}}) = C\int_0^{\infty} \mathrm{d}\lambda \varepsilon(\lambda)\varepsilon_{\text{atm}}(\lambda) I_{\text{BB}}(T_{\text{amb}}, \lambda) = C\int_8^{13} \mathrm{d}\lambda \varepsilon_{\text{atm}}(\lambda) I_{\text{BB}}(T_{\text{amb}}, \lambda) \tag{8}$$

$$P_{\text{rad}}\left(T_{\text{eq}}^{\text{se}}\right) = C\int_0^{\infty} \mathrm{d}\lambda \varepsilon(\lambda) I_{\text{BB}}\left(T_{\text{eq}}^{\text{se}}, \lambda\right) = C\int_8^{13} \mathrm{d}\lambda I_{\text{BB}}\left(T_{\text{eq}}^{\text{se}}, \lambda\right) \tag{9}$$

Similarly, equilibrium is achieved when $P_{\text{atm}}(T_{\text{amb}}) = P_{\text{rad}}(T_{\text{eq}}^{\text{se}})$, where $T_{\text{eq}}^{\text{se}}$ is the steady-state temperature of the ideal selective emitter. It can be found that $T_{\text{eq}}^{\text{se}} < T_{\text{eq}}^{\text{BB}}$ because the blue line is beneath the black line of blackbody radiation. Hence, an ideal selective emitter can reach a lower equilibrium temperature than a blackbody. Moreover, for a selective radiator, this holds to be true even if taking solar irradiance and nonradiative heat transfer into account, as long as we change the steady-state condition into $P_{\text{cool}}(T_{\text{eq}}^{\text{se}}) = 0$. It is because the ideal emitter can reflect all the solar radiation while a blackbody strongly absorbs sunlight, and the nonradiative heat transfer is negligible if we thermally insulate the emitter. Since thermal emissivity has a maximum value, $\varepsilon(\lambda) = 1$, it is suggested that even an ideal selective emitter has an upper bound for the cooling power and a lower bound of attainable temperature. As calculated by Rephaeli et al.,[8] the maximum power for radiative cooling is about 150 W m^{-2}, and the minimum temperature is around 195 K.

3. High Emission Devices for Nighttime Radiative Cooling

From the previous section, we know that a blackbody emitter can realize radiative cooling during the night, and if we can control the emitter's spectrum, much better performance will be obtained. Many efforts have been devoted to the development of selective radiation after the first detailed discussion presented by Head in 1959.[9] At the early stage, a variety of works have demonstrated different methods for radiative cooling. Most of them concentrated on designing selective emitters that primarily emit radiation in the atmospheric transparency window. These designs achieved sizable cooling effects at night, including polymer films, inorganic films, pigment paints, and ammonia gas.[10]

3.1. Polymer Films

Many polymer films show broad intrinsic selectivity in the infrared range, matching the atmosphere window. Therefore, certain plastic coatings have been investigated and used as selective emitters. Since most of the polymer films are fairly transparent elsewhere in the spectrum, emitters are often constructed with the polymer films placed on aluminum sheets, a metallic substrate with high reflectance. This design is especially useful in the real application, because the path of light in the polymer doubles due to the reflection, maximizing the light absorption of the polymer film.

A comparison of various polymer coatings has been conducted by Granqvist et al.[4] and extracted in **Figure 3**.

In the work of Trombe,[11] polyvinylchloride (PVC) films were explored for radiative cooling (Figure 3a). The spectrum of a 100 μm thick PVC film is shown in Figure 3b, which corresponds to a 50 μm thick PVC film placed on the aluminum sheet. Though the selectivity was weak, this emitter achieved a radiative cooling below the ambient temperature at nighttime.

Tedlar, a polyvinyl-fluoride plastic, was demonstrated as another efficacious radiative cooling material by Catalanotti et al.,[7] Bartoli et al.,[14] and by Grenier.[12] The device was built by coating evaporated aluminum onto a 12.5 μm thick Tedlar film. The device had an average reflectivity of 0.1–0.2 inside the transparency window and a reflectivity of ≈0.85 outside (Figure 3c). This is a quite good infrared selectivity comparing to that of a PVC film. In their experiment, Catalanotti et al.[7] obtained a net cooling power of ≈50 W m^{-2} at ambient temperature during the night and a net cooling power of 20 W m^{-2} in the daytime with shielding against direct sunlight.

Figure 3d depicts a spectrum profile for a 340 μm thick TPX film, as proposed by Grenier.[12] The infrared selectivity is evident, and the nocturnal cooling performance of this film is manifest, about the same as the Tedlar film.

The polymer film radiator has an advantage over other materials due to its scalability, which enables its large-scale manufacturing and practical use. However, its moderate intrinsic selectivity limits the diurnal cooling performance, and a relatively high absorption in the solar spectrum eliminates its cooling effect under direct sunlight.

3.2. Inorganic Films

A significant absorbance peak in the middle of the atmospheric transparency window is the characteristic feature of silicon

© 2020 WILEY-VCH Verlag GmbH & Co. KGaA, Weinheim

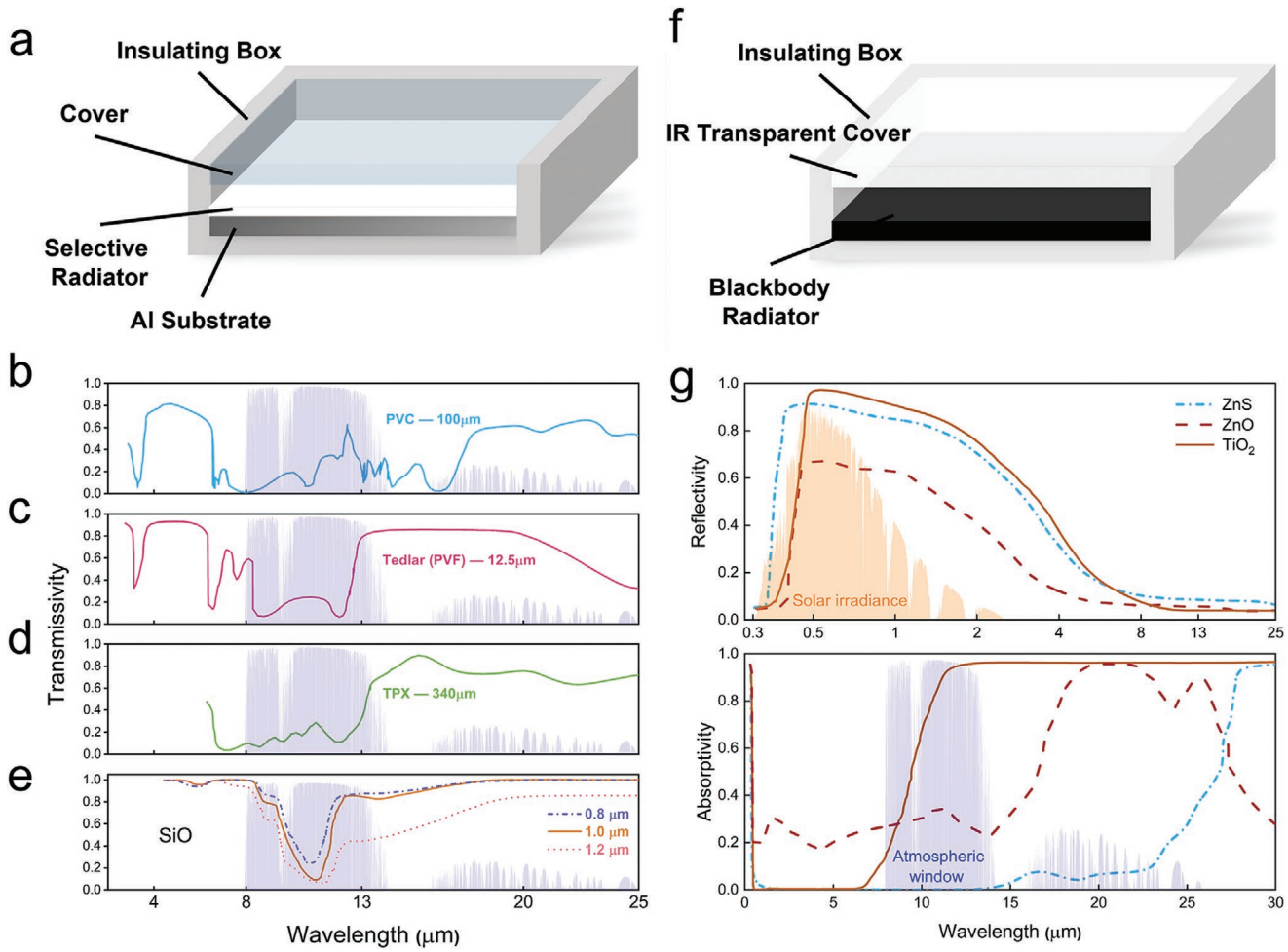

Figure 3. a) Schematic drawing of a typical experimental selective emitter. b–d) Transmittance spectrum for three different plastic films of interest for radiative cooling, which is reproduced from works of Trombe,[11] Catalanotti et al.,[7] Grenier,[12] and Granqvist and Hjortsberg.[4] Reproduced with permission.[4] Copyright 1981, AIP Publishing. e) Transmittance spectrum of SiO films with different thicknesses. Reproduced with permission.[4] Copyright 1981, AIP Publishing. f) Schematic drawing of a typical experimental two-layered structure with selective cover and blackbody emitter. g) Calculated total reflectance and total absorptance spectrums for different pigment particles in polyethylene foils. Reproduced with permission.[13] Copyright 1995, Elsevier.

monoxide (SiO) and other inorganic compounds such as silicon nitride (Si_3N_4) and magnesium oxide (MgO). Take the case of SiO: its absorptivity peak, also known as the emissivity peak, at 10 μm is physically caused by silicon-oxygen stretching modes. This is why earlier literature chose silicon-based materials as infrared selectivity emitters. In addition, for the same reason as mentioned in the previous section, the device was constructed by depositing SiO film onto an aluminum substrate. The surface roughness of the metal substrate had an influence on the broadband emissivity, and a thermal emissivity around 0.05 is typical for commercial aluminum surface.

The curve of Figure 3e refers to thickness-dependent spectrums of SiO films which are replotted from Granqvist and Hjortsberg[4] in 1981. As the thickness increases, the reflectance progressively decreases, especially outside the atmospheric window at 13–20 μm. Therefore, a certain thickness of about 1 μm is recommended for a better performance of the emitter. The radiator with 1 μm thick SiO film has a desired steep dip in the 8–13 μm spectral range and has nearly 100% reflectance at longer wavelengths. The selectivity is superior to that of the polymer films mentioned above, and the silicon monoxide device can reach a cooling power around 60 W m^{-2} during the night. Notably, the strong thickness dependence of the reflectance curves indicates that interference effects are consequential in determining the spectral reflectance. The interference effects are quite useful in modulating the spectral reflectance of specific emitters in narrowband, which have been comprehensively explored in recent works.

Proposed by Granqvist et al.[15] in another work, silicon nitride films share similar spectrum reflectance as silicon monoxide because of the resemblances between nitrogen and oxygen. Besides SiO and Si_3N_4, a series of silicon-based materials such as silicon oxynitride (SiO_xN_y),[15–17] SiC, and SiO_2 nanoparticle resonators[18] also show infrared selectivity.

Single-crystal magnesium oxide (MgO) also has favorable optical properties as a selective emitter. As demonstrated in the work of Berdahl,[19] a 1.1 mm thick polished MgO film or a 0.54 mm thick lithium fluoride (LiF), backed with an aluminum layer, could reach lower temperatures than PVF films. An equilibrium temperature of 20 K below ambient was detected.

© 2020 WILEY-VCH Verlag GmbH & Co. KGaA, Weinheim

3.3. Pigment Paints

Apart from the film structure emitter, another available choice for nocturnal radiative cooling is pigment paint. Many of the oxides and carbonates of titanium, aluminum, calcium, and zinc present high emissivity in the atmospheric window and possess high reflectivity in the visible region. A lot of white paints contain these compounds. The high reflectivity in the visible region helps to block solar radiation, which is a conducive feature for daytime radiative cooling. Though these materials failed to perform diurnal cooling phenomenon, they imply suggestively a feasible way to achieve that. Additionally, the flexibility of paints provides them versatility in real-world applications.

Harrison and Walton[20] first studied radiative cooling paints that contain titanium dioxide (TiO_2). Commercial white paint with 35% of TiO_2 was selected for the test of cooling power, and a maximum of 15 °C temperature drop was obtained, which was significant. It is worth noting that the experiment was conducted at an altitude of 1.1 km, so performance might be degraded at a lower height or in a more humid climate. Later, Orel et al.[21] stated that by adding $BaSO_4$ into TiO_2 pigment paints, the cooling performance could be promoted even further.

In further studies, inspired by the work of Addeo et al.,[22] a different idea from selective emitter has been put forward for radiative cooling. Rather than treating the pigments or thin films themselves as selective radiators, Nilsson et al.[13] used a selective infrared transparent cover that could reflect most of the sunlight and broadband thermal radiation, along with a blackbody radiator dwelled beneath the cover (Figure 3f). The difference in Addeo et al.'s work[22] is that the conventional selective emitter is directly exposed to the environment, while the cover in this device serves as a selective shield that blocks unwanted radiation away from the blackbody emitter. Thereby, the requirement for selective cover's absorption properties in the atmospheric window is inverse for that of selective emitter's. At the same time, both the selective emitter and the cover should have high reflectivity outside the window. The optical spectrums of different pigments, including ZnS, ZnO, and TiO_2, are extracted and shown in Figure 3g. A maximum cooling power of ≈100 W m^{-2} was measured, and as Nilsson et al.[13] stated that the cooling effect was achieved all day except for the 4.5 h around noon.

4. Integrated Devices for Daytime Radiative Cooling

Previous literature focusing on nocturnal radiative cooling mainly devoted their efforts to improving the radiator's emissivity in 8–13 μm range and hence the nighttime performance of cooling. By contrast, few were trying to promote cooling, or at least avoid heating in the daytime. Because simultaneous high emissivity in the infrared range and high reflectivity outside the range is not easily achieved, a tradeoff is seemingly unavoidable. All the attempts to achieve daytime radiative cooling at that time failed, given that the power of solar radiance is not a small number, and a little increase in the absorption of sunlight will lead to apparent heat inflow P_{sun}, a number significant enough to overwhelm the power radiated out, P_{rad}. Only with a strong selectivity over the whole optical spectrum can the emitter satisfy the strict restrictions of daytime radiative cooling.

Quantitatively, normal solar irradiance (AM1.5 Global Tilt spectrum) is nearly 1000 W m^{-2},[8] while most of the nocturnal radiative cooling devices have maximum net cooling powers of no more than 100 W m^{-2}. This is to say that little cooling effect or even heating phenomenon will occur with an average of 0.9 reflectivity equating to just 0.1 absorptivity in the solar spectrum. In recent years, the blossoming of many modern tools of optics and photonics has enabled a more extensive spectral control over thermal radiation. For the first time, substantial daytime radiative cooling was reported by Fan's group in 2014,[1] and a lot of work following has made daytime radiative cooling an emerging field.

4.1. Nanophotonic Approach for Daytime Radiative Cooling

The nanostructures of photonic materials render them novel optic properties in addition to their inherent characteristics. While intrinsic bulk materials often radiate over a broad spectrum, photonic materials can be utilized to design a thermal source with a controlled, narrowband emission spectrum, which is particularly desired in radiative cooling.

The basic concept here is to control spectral thermal emission using Fabry–Pérot interference. An interference structured material uses two parallel reflecting surfaces, which typically are consisted of a thin metallic film and a mirror substrate and separated by a thin transparent layer to obtain large absorption/emission. To illustrate the principle for control over emission, we will take high absorptance 1D photonic emitter as an example. A beam of light passes through the thin metallic film and streams into the transparent layer, the multiple reflections between the two reflecting surfaces interfere with themselves. Destructive interference occurs if the transmitted beams are out of phase. In this way, a beam of light with a certain frequency is "trapped" or "consumed" in between the two surfaces, and thus the material presents high absorption at this wavelength. If we replace the thin metallic film with a small disk array, which is common in 2D photonic design, the interference frequency bandwidth will broaden, and the emitter will show high absorption to quasi-monochromatic light. A similar process due to constructive interference has been established for high transmittance photonic materials. Therefore, we can extensively operate on the optical properties at any wavelength by fabricating a transparent layer with a specific thickness, and we can use a combination of different sets of emitters to take control over the whole spectrum.

With the development of nanophotonic techniques, many nanostructured materials have been investigated and utilized in radiative cooling, including layered systems, metasurfaces, and microsphere-based random materials.

The original work of Rephaeli et al.[8] in 2013 presented a calculation result that an ultra-broadband photonic structure could achieve daytime radiative cooling. As shown in **Figure 4**a, the emitter was constructed by two parts. On the top, two 2D photonic crystal layers consisted of SiC and quartz with periodically etched

© 2020 WILEY-VCH Verlag GmbH & Co. KGaA, Weinheim

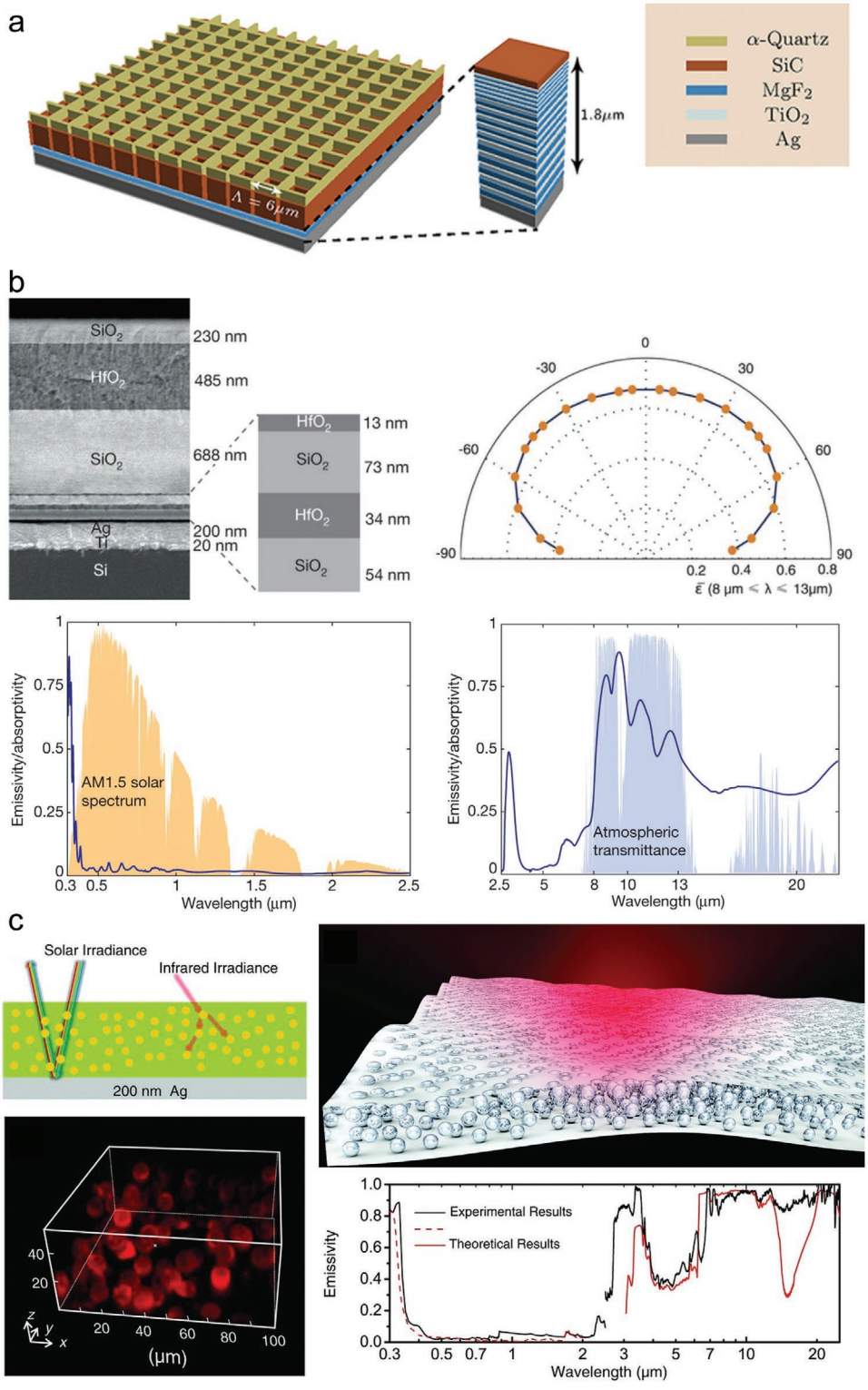

Figure 4. a) Daytime radiative cooler design that consists of two thermally emitting photonic crystal layers comprised of SiC and quartz, below which lies a broadband solar reflector. Reproduced with permission.[8] Copyright 2013, American Chemical Society. b) Scanning electron microscope image of the photonic radiative, average measured emissivity plotted as a function of polar angle of incidence and measured emissivity/absorptivity of the photonic radiative cooler over optical, near-infrared wavelengths and mid-infrared. Reproduced with permission.[1] Copyright 2014, Springer Nature. c) A schematic of the polymer-based hybrid metamaterial with randomly embedded SiO_2 microsphere for large-scale radiative cooling, confocal microscope image of the hybrid metamaterial, and the emissivity/absorptivity of the 50 mm thick hybrid metamaterial from 300 to 25 mm. Reproduced with permission.[2] Copyright 2017, The American Association for the Advancement of Science.

© 2020 WILEY-VCH Verlag GmbH & Co. KGaA, Weinheim

square air holes could provide surface phonon–polariton resonances in the 8–13 μm range, and thus can serve as selective emitters in the atmospheric window. On the bottom was a solar reflector made of chirped 1D photonic crystal with three sets of five bilayers placing on a silver substrate, which covered the entire solar spectrum. Inspiringly, the calculation showed that in an optimized situation, the emitter could reach a net cooling power over 100 W m^{-2} under direct sunlight.

Raman et al.[1] first experimentally demonstrated substantial daytime radiative cooling effects, using an integrated planar layered 1D photonic crystal. Analogical to the previous calculation work, the emitter here was composed of two parts. The upper three thick alternating hafnium dioxide (HfO_2) and silicon dioxide (SiO_2) layers were tested to have high emittance in the atmospheric window through a combination of intrinsic properties and structure effects, and the lower four thin layers had a strong reflection to solar radiation. The emitter was stacked on top of 200 nm silver (Ag) reflector. As shown in Figure 4b, the emitter reflected 97% of incident sunlight and possessed a manifest selectivity in the infrared range. Another key point for improving cooling power is enabling broad-angle emission. Many photonic crystals exhibit directivity, showing nonuniform angular distributions of emission. Nonetheless, this radiator persisted emissivity to 60° from zenith, a remarkable feature to enlarge power radiated out P_{rad}, see Equation (2). As reported, the cooling device could generate a power of 40.1 W m^{-2} at ambient air temperature and could cool to 4.9 °C below ambient when exposed to direct sunlight.

Many other published systems also achieved daytime cooling with multilayers 1D photonic crystals. For example, Gentle and Smith[23] developed an open surface cooling device with multiples of polymer pairs, composed by one with high index and the other with low index. The polymer pairs exhibited similar reflecting phenomena as metallic mirrors in photonic crystals by which optical properties were modulated. A later optimized device designed by Chen et al.[24] achieved subfreezing temperatures in a 24 h cycle. Two layers emitter containing silicon nitride (Si_3N_4) and amorphous silicon (Si) along with a selective ZnSe window was exploited.

It is also valid to use 2D photonic crystals as selective emitters. Hossain et al.[25] theoretically investigated metamaterial for daytime radiative cooling, and an array of symmetrical conical metamaterial (CMM) pillars was used. As depicted, the 2D CMM structure led to nearly unity emissivity matching the entire 8–13 μm window, and for wavelength larger than 16 μm, the CMM material behaved like a metallic mirror with an absorptivity of smaller than 0.1. The point here was to diminish the atmosphere radiation. However, the CMM structure intensively absorbed solar light, and thus infrared radiation (IR) transmitting solar reflector was needed. A photonic crystal cover could reflect 97% of solar light. This paper stated a cooling power of 116.6 W m^{-2} in the ideal condition, whereas in the real-world application, the power might be lower. The cover should be entirely transparent to infrared radiation, or else the effective emissivity of the whole device would be at a discount.

Further, Zhu et al.[26] illustrated a concept that radiative cooling could be used in combination with the solar absorber. The solar absorber was deposited on a 500 μm thick 2D silica photonic crystal and performed a cooling effect of 13 °C lower than bare absorber. Besides, Wu et al.[27] demonstrated that a temperature-dependent power-switchable cooling device could be obtained based on VO_2-coated silicon microcones 2D photonic crystal. This VO_2-coated crystal had a phase-change behavior around 330 K, which was inspiring for dynamic modulating radiative cooling and thermal management.

Recent nanophotonic researches have yielded remarkable progress compared to the past. Substantial daytime radiative cooling has been accomplished and applied in various scenarios. A variety of designs comprised dielectrics, polymers, and polymer-dielectric photonic crystals. Though these designs presented a high efficiency on radiative cooling, they were costly and vulnerable. Most of them were fabricated on a small scale by photolithography or electron beam evaporation with prolix procedures and needed to be shielded with bulky shells and covers. Also, because most of the photonic materials are translucent, in order to obtain high solar reflection, they need to be deposited on metal mirrors. Therefore, seeking more straightforward approaches and more scalable radiative cooling materials is necessary.

4.2. Scalable Approach for Daytime Radiative Cooling

Though efficient cooling performance has been achieved via photonic crystals, most of them are expensive or fragile, therefore limiting their applications. On the other hand, materials such as paints or polymer films are easy to preserve, transport, and apply in different textures and geometries. Without appurtenances these materials can serve as radiators, making them appealing candidates for real-world use.

A high-throughput, economical roll-to-roll method for daytime radiative cooling was proposed by Zhai et al.[2] in 2017. Here, they fabricated a 50 μm thick polymethylpentene film (TPX) encapsulating random-distributed 8 μm diameter SiO_2 microspheres (Figure 4c) as a metamaterial selective emitter, since the phonon resonances of SiO_2 microparticle could enhance its thermal emissivity to more than 0.93. Moreover, both TPX and SiO_2 microparticles are transparent to solar light, avoiding the heat from the sun. It needs to be mentioned that the diameter of the SiO_2 microspheres exclusively influenced the optical properties of the metamaterial. For instance, large microspheres had strong absorption in both solar and infrared spectrum whereas smaller microspheres resulted in sharp resonance and reduced the overall emission. When the metamaterial film was coated on a silver reflector, this device captured only 4% of sunlight.

Inspired by previous cool-roof paints (CRPs), Mandal et al.[3] replaced the dielectric pigments, such as Zinc oxide in CRPs, with light-scattering air voids, as seen in **Figure 5**a. They developed an inexpensive hierarchically porous polymer $P(VdF\text{-}HFP)_{HP}$ coating for daytime radiative cooling. $P(VdF\text{-}HFP)_{HP}$ absorbs negligible sunlight intrinsically and has multiple emission peaks arising from different vibration modes of its molecular structure. Hence, a superb selectivity (solar reflectance of 0.96 and infrared emittance of 0.97) and a broad-angle uniformity were demonstrated, which eliminated the need for metal reflectors that was common for photonic crystals. Moreover, $P(VdF\text{-}HFP)_{HP}$ is durable to weathering, contaminating, and UV radiation. When placed outdoor, it can remain its optical properties nearly unchanged for a long time.

© 2020 WILEY-VCH Verlag GmbH & Co. KGaA, Weinheim

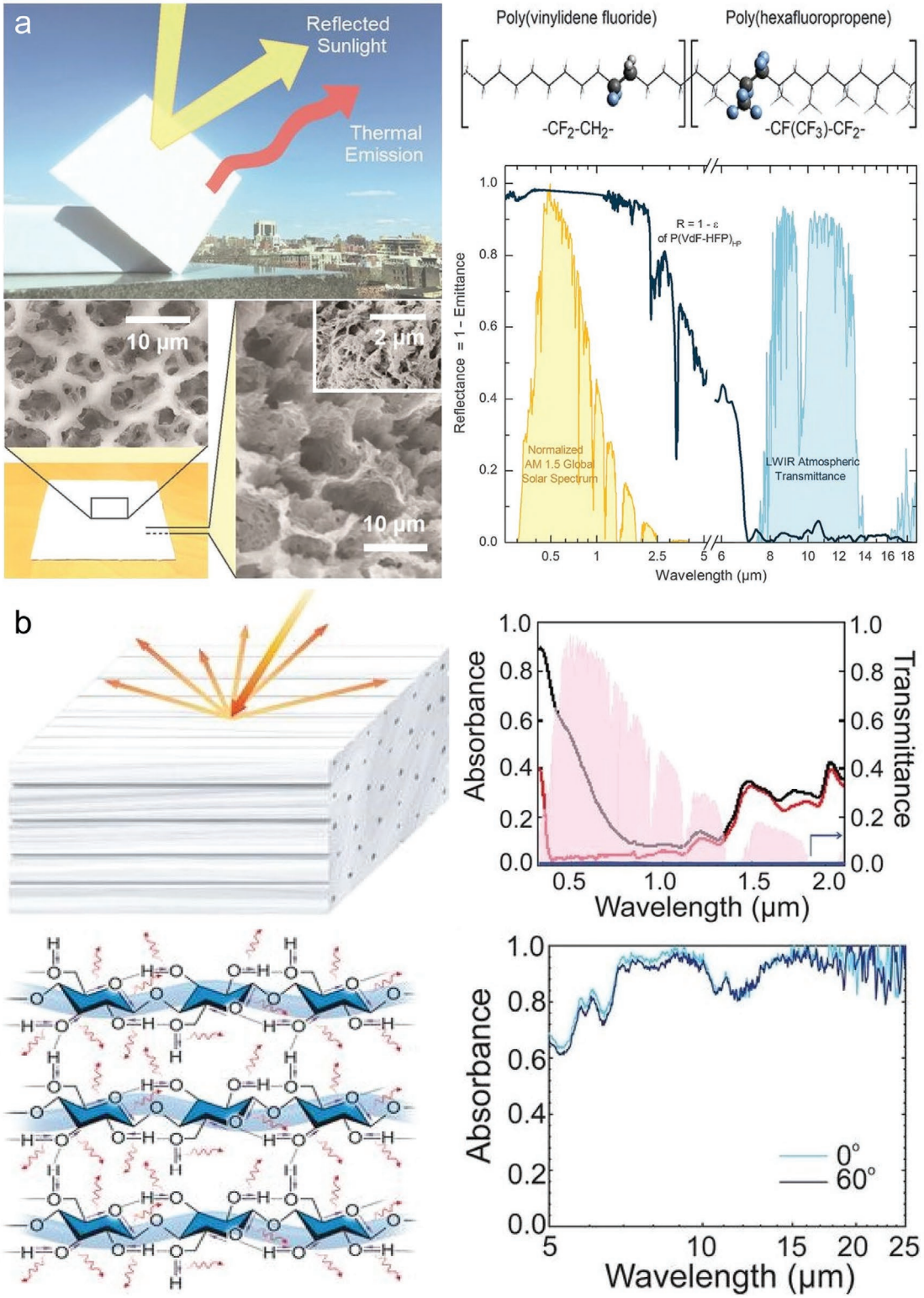

Figure 5. a) Photograph superimposed with schematics to show that high reflection of solar and emittance of IR enable a net radiative loss and passive daytime radiative cooling, micrographs showing top and cross-section views of P(VdF-HFP)HP, spectral reflectance of a 300 mm thick P(VdF-HFP)HP coating and the LWIR atmospheric transparency window. Reproduced with permission.[3] Copyright 2018, The American Association for the Advancement of Science. b) Left: Schematic showing the wood structure strongly scattering solar irradiance and schematic of infrared emission by molecular vibration of the cellulose functional groups. Right: Absorption of the natural and cooling wood in the solar spectrum and Infrared emissivity spectra of the cooling wood between 5 and 25 mm at different emission angles. Reproduced with permission.[28] Copyright 2019, The American Association for the Advancement of Science.

© 2020 WILEY-VCH Verlag GmbH & Co. KGaA, Weinheim

Li et al.[28] engineered wood and rendered a scalable structural material, achieving daytime radiative cooling with the desired size and mechanical features for construction. Due to the emission of OH and stretching vibration modes of C–H, C–O, and C–O–C (Figure 5b), the wood exhibited high broadband emission from 8 to 13 μm. The rough surface of wood, on the other hand, could scatter most incident light and render high solar reflectance. A pronounced impact of cooling was shown in dry climates. The surface was also hydrophobic after fluorosilane treatment, and hence could provide buildings with more protections against humid weather.

In summary, the emerging materials and technologies enabled excessive integrated control over optical properties. As a result, the cooling performance escalated over time and the choices of emitters enriched for different purposes. More specifically, robust daytime radiative cooling has been achieved by various engineering approaches, including designing nanostructured and microstructured photonic crystals or applying simple and scalable approaches based on polymer materials. To improve the rate of cooling, people have made great efforts on operating optical properties. Meanwhile, some previous work also counted in the influence of parasitic heat loss and atmosphere conditions for further temperature reduction.

5. Optimization of Radiative Cooling Performances

As shown in Equation (1), the net cooling power is determined by four key components: the power radiated out P_{rad}, the thermal radiation absorbed from the atmosphere P_{atm}, the radiation power received from solar light P_{sun}, and the parasitic heat loss $P_{cond+conv}$. As P_{sun} and P_{atm} have been detailed discussed in preceding sections, here we will focus on suppressing the parasitic heat loss to optimize the daytime cooling performance at a system level, and on analyzing the weather's influences on the outcoming power P_{rad} to gain a more thorough understanding of daytime radiative cooling.

5.1. Parasitic Heat Losses

Usually, the heat loss is composed of conduction and convection, and minor radiation from the backside of the emitter is also accounted for to provide a precise calculation. For simplicity, we denote the parasitic heat loss as $P_{cond+conv}$. Parasitic heat load will have a manifest impact on net power if we do not take measures to eliminate the loss. For example, an emitter placing on a metallic substrate probably gains no actual temperature reduction, since the high-conductivity substrate will transfer heat and balance the cooling effect. Besides, when an emitter is exposed to the windy external environment, the emitter will be heated through convection and conduction by the warm airflow. Thus, it is essential to minimize the parasitic heat loss to approach the power limitation of radiative cooling.

We use the case taken from Chen et al.'s work[24] to evaluate the parasitic heat loss quantitatively. Suppose an ideal selective emitter is placed in a device and has thermal contact with the outside through conduction, convection, and radiation. Absorption of sunlight is dismissed because of the complete reflection in the solar spectrum, which means the thermal balance is determined only by three factors (**Figure 6**a)

$$P_{cool}(T) = P_{rad}(T) - P_{atm}(T_{amb}) - P_{cond+conv} \quad (10)$$

Here the parasitic heat loss is characterized by heat transfer coefficient h as in Equation (5). Parasitic heat loss is proportional to h, therefore, $h = 0$ W m^{-2} K represents perfect thermal insulation, while a typical experimental value is $h = 8$ W m^{-2} K. Figure 6b depicts the h dependence of cooling performance for several different materials. As seen when the parasitic heat loss is eliminated, the steady-state temperature of an ideal selective emitter is 60 °C below ambient. However, the temperature reduction declines to less than 10 °C when h raises to 8 W m^{-2} K.[24] From Equation (11), we can also conclude that parasitic heat loss has no impact on cooling performance at ambient temperature.

Figure 6c illustrates a thermal insulating apparatus[24] that is designed to accomplish ultra-low parasitic heat loss. First, the emitter is installed in a vacuum chamber to minimize the air conduction and convection. Second, when the sample is put on four pegs, the backside heat conduction is restricted to an extremely low level. Third, the encompassing reflective radiation shields and mirror-cone prevent incoming atmosphere radiation and diffused sunlight except for the zenith direction, and the shade standing vertically aside covers up the direct sunlight for the chamber. In addition, the anti-reflection ZnSe window is transparent in the IR range. Such an apparatus ensures that the emitter thermally decouples from the surrounding environment and only couples to the outer space through the atmospheric transparency window.

Though this apparatus is of little practical use in real-world applications, it shows an optimized performance for a radiator and a remarkable subfreezing temperature is achieved. The result of a continuous 24 h experiment is presented in Figure 6d. The temperature of the selective emitter was tracked with the trend of the ambient temperature and found to be maintained at 35 °C lower than ambient in a day–night cycle, proving the efficacy of the solar shade and the radiation shields. Notably, the nadir of the sample's temperature occurred at noon with peak solar irradiance. This counterintuitive fact arose from the mismatch between ambient air temperature and the dew point.

Many reported radiative cooling devices had been equipped with thermal insulation to restrain the heat loss and, though are much more modest than the apparatus mentioned above, do promote the net cooling power. As presented by Leroy et al.,[30] polyethylene aerogel (PEA), a thermally insulating material, could be placed on top of the emitter as a cover. Moreover, the PEA materials were solar-reflecting and infrared-transparent, which could reduce solar absorption. The PEA cover could be integrated with existing emitters to improve the cooling performance. Experiment results showed that PEA emitter could reach an equilibrium temperature of 10 °C lower than no-PEA device.

5.2. Weather Impacts on Cooling Performance

Weather conditions greatly influence the emitter's radiation power. Emitter radiates heat out by thermally coupled to the universe through an atmospheric transparency window. Previously,

© 2020 WILEY-VCH Verlag GmbH & Co. KGaA, Weinheim

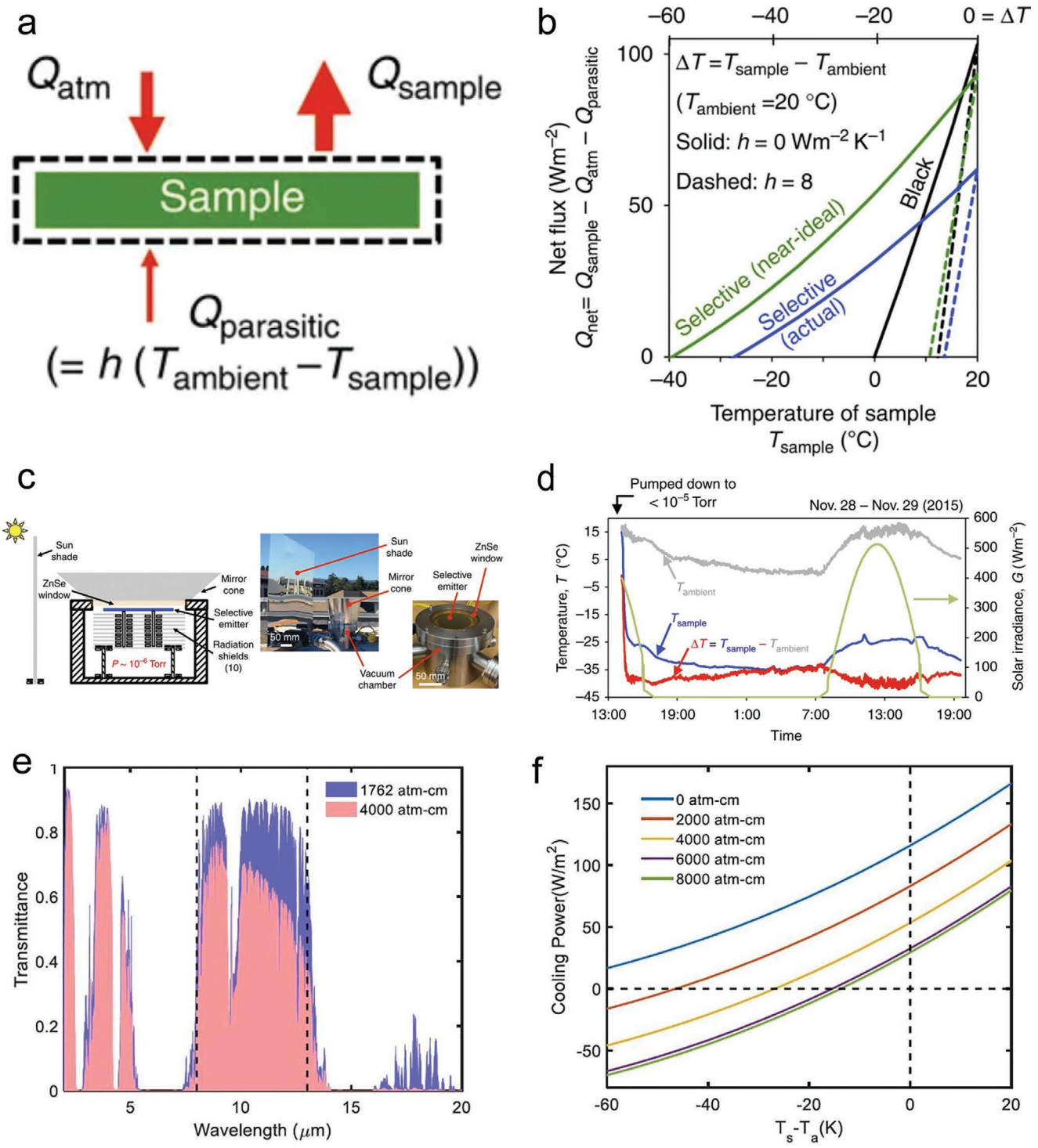

Figure 6. a) Energy balance applied to the radiative emitter. b) Net flux as a function of the temperature of the sample. c) Schematic and photograph of in situ experimental setup. d) Large temperature reduction below ambient through radiative cooling in a 24 h day–night cycle. Reproduced with permission.[24] Copyright 2016, Springer Nature. e) Modeled atmospheric transmittance for US (TWC = 1762 atm cm) and Shanghai summer weather (TWC = 4000 atm cm) in the cloud-free day. f) The cooling performance for ideal selective emitter for different total water vapor column with T_{atm} = 298 K and h = 0 W m^{-2} K. Reproduced with permission.[29] Copyright 2019, Elsevier.

in the discussion of P_{rad}, we made an unstated assumption that the atmosphere transparency on the ground is ideal all the time. However, it can only be obtained under a clear and dry sky in reality. In practice, the atmosphere transparency is sensitive to both air humidity and clouds amount, and therefore, the outcome radiation power varies with changes in weather.

© 2020 WILEY-VCH Verlag GmbH & Co. KGaA, Weinheim

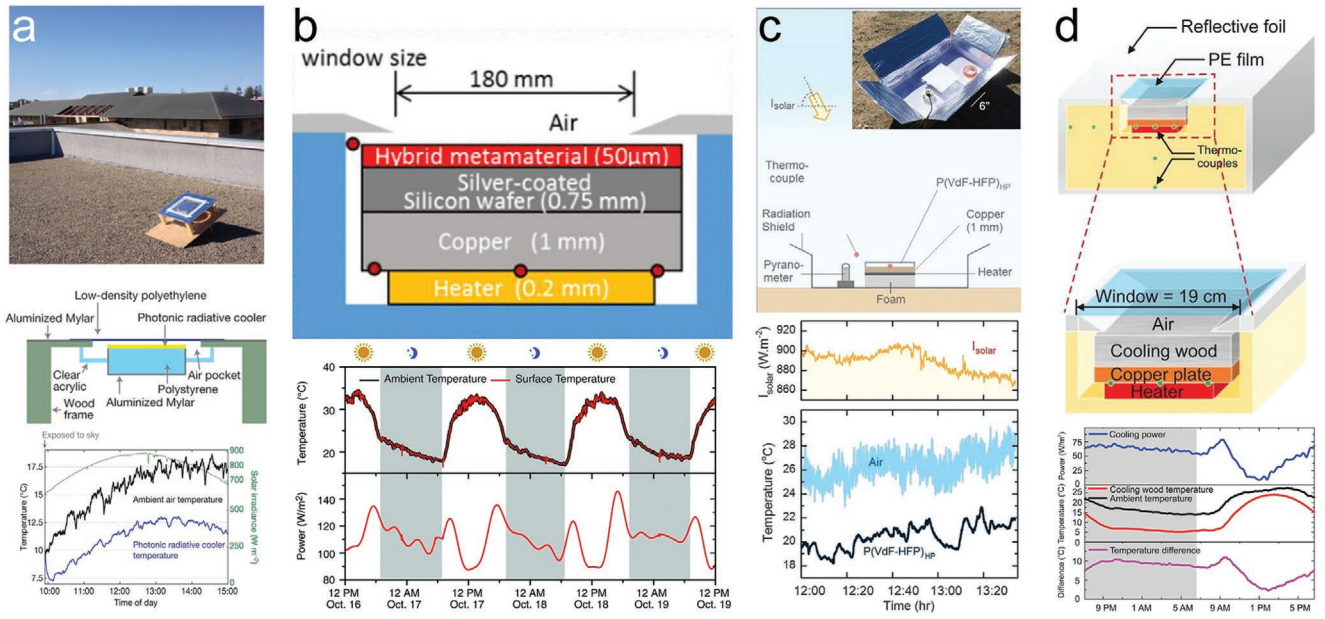

Figure 7. a) Schematic and photograph of experimental setup and measurement of the photonic radiative cooler's performance. Reproduced with permission.[1] Copyright 2014, Springer Nature. b) Schematic of the setup and measurement of temperature and radiative cooling power over 3 days. Reproduced with permission.[2] Copyright 2017, The American Association for the Advancement of Science. c) Schematic of the setup for testing performance under sunlight and temperature data of the result. Reproduced with permission.[3] Copyright 2018, The American Association for the Advancement of Science. d) Schematic of the thermal box used to characterize the radiative cooling power and cooling temperature and measurement of the 200 mm × 200 mm cooling wood. Reproduced with permission.[28] Copyright 2019, The American Association for the Advancement of Science.

Atmosphere transparency depends particularly on humidity because of the water vapor's strong emission around 6.3 and 20 μm. Figure 6e extracted from Liu et al.'s work[29] shows an apparent discrepancy in transmittance between the US and Shanghai, where transmittance is much higher in the dry area than in the moist area. Here the absolute humidity is represented by the total water vapor column (TWC), which is a measure of the total water vapor contained in a vertical atmosphere column. An intuitive view of the relationship between humidity and cooling power is sketched in Figure 6f for an ideal selective emitter, calculated based on the simulation by MODTRAN.[31] As the humidity increases, the cooling power rapidly goes down. The descending trend is even more evident in experiments, as seen in a comparison of works between Raman et al.[1] and Tso et al.[32] Hence, accounting the impact of humidity, it is recommended to apply the radiative cooling devices in arid areas.

5.3. Experimental Device Design for Daytime Radiative Cooling Performances Test

For a radiative cooling device, two important metrics are indicative of evaluating the performance. First is the net power P_{cool}. The net cooling power is correspondent to the device temperature one to one and the most commonly used one is the power at ambient, $P_{cool}(T_{amb})$. In the experiment, $P_{cool}(T_{amb})$ is defined by the input power of the heater that keeps the device at ambient temperature. Second is the steady-state temperature T_{eq}, the lowest temperature a cooler can reach without heat input, when $P_{cool} = 0$. Notably, for comparisons in different cooling devices, higher net power at ambient is not strictly linked to a lower steady-state temperature, according to the different spectral properties and the different heat transfer coefficients.

Here we summarize the performances of several cooling systems mentioned above. The cooling system built by Raman et al.[1] was composed of a planar photonic crystal surrounding by an air pocket to reduce the heat loss and was tilted 30° toward the south to face the solar radiation directly. The curves in **Figure 7**a demonstrate the coolers' temperature in a daytime interval. The cooler approximately achieved a T_{eq} of 4.9 °C below ambient when the solar irradiance was at peak.

Zhai et al.[2] placed a scalable hybrid metamaterial in a half-open radiation shield (Figure 7b). A closed-loop heater kept the cooler's surface temperature the same as the air outside, so that the parasitic heat loss was naturally eliminated without thermal insulation. A continuous measurement over three days presented an average power of about 110 W m^{-2}, close to the power limitation of 150 W m^{-2} mentioned in the previous section.

Mandal et al.[3] proposed another half-open system for radiative cooling (Figure 7c). The sample was placed on a copper film in contact with the heater to ensure the heat transfer. Foams and radiation shields were used to eliminate heat loss. An average temperature reduction of about 6 °C over the duration of the experiment was demonstrated. Besides, in a temperature tracking experiment, an average net power of 100 W m^{-2} was shown.

A similar system was also employed in work conducted by Li et al.,[28] as shown in Figure 7d, with the cooling-wood

© 2020 WILEY-VCH Verlag GmbH & Co. KGaA, Weinheim

dwelling in the thermal box. Steady-state temperature and net power were tested simultaneously in two boxes. It is obvious that cooling power and temperature difference obeyed the same trend, consistent with the near-linear relation depicted in Figure 6b.

We will conclude this section by pointing out that recent devices have already achieved efficient cooling effects of practical meaning and are approaching the upper net power limit. It is appealing to apply the abundant energy of radiative cooling in real-world applications.

6. Potential Real-World Applications of Daytime Radiative Cooling

Daytime radiative cooling is emerging as a promising method of complementing traditional cooling systems (such as AC) to reduce cooling energy consumption. It is expected that passive radiative cooling materials and systems can be applied in different scenarios, such as cooling systems in energy-efficient buildings, personal thermal management, etc. This section will summarize and discuss recent reports about daytime radiative cooling materials, devices, systems and their applications.

6.1. Buildings

Cooling is a high-energy-consuming practice but necessary for modern societies. Among all, ≈40% of the energy used in buildings is on conventional heating, ventilating, and air-conditioning systems (HVAC).[33] On the contrary, passive cooling techniques can cool objects without power input, which significantly reduce the energy consumption (**Figure 8**a).

Zhai et al.[2] demonstrated a high-throughput, economical roll-to-roll method of producing polymer metamaterial. With the lightweight and outstanding flexibility, the polymethylpentene (TPX) can be used as the cover of the building's exterior. In addition, TPX has excellent mechanical and chemical resistance, which offer a long-lifetime potential. By using the roll-to-roll preparation method, the TPX can be produced at a rate of 5 m min^{-1}. All of the advantages make the TPX metamaterial a promising application in daytime radiative cooling building (Figure 8b). Another polymer-based radiative cooling material was presented by Mandal et al.[3] They reported a simple way to fabricate hierarchically porous poly(vinylidene fluoride-*co*-hexafluoropropene) [P(VdF-HFP)HP] coatings. The coatings were freestanding sheets with a paint-like applicability. For instance, it can be painted, dip-coated, or sprayed onto various substrates like metal, plastics, and wood. This feature allows [P(VdF-HFP)HP] coatings to be used widely as the exterior building paint (Figure 8c).

Besides polymer-based materials, Li et al.[28] designed cooled wood with a superior mechanical strength (404.3 MPa) about 8.7 and 10.1 times the strength and toughness of natural wood, which can be potentially used as materials for building construction. Cellulose nanofibers in the cooling woods can backscatter solar radiation and strongly emit mid-infrared wavelengths, so materials can be continuously cooled below ambient temperature both day and night (Figure 8d). Li et al.[28] selected 16 cities in the United States as representatives of various residential areas and built models using the cooling wood as the roof. Results showed the cooling roof could save 20–60% of energy.

Typically, there are three models of radiative cooling systems (air-based, water-based, and hybrid systems) that are commonly accepted.

6.1.1. Air-Based Systems

In air-based cooling systems, the air is the heat-exchange media, which transfers heat between the environment and the radiator.[35,36] Fans or natural process, due to the buoyancy effect, can drive the air to maintain the heat-exchange process. Air-based systems have the advantages of being cheap and straightforward to install.[37] Nevertheless, it is hard to implement and integrate these systems into buildings, because they can only be adopted in a detached house, the top floor of a duplex, or a multi-story building. Moreover, the radiator must have air channels with a large enough surface area to maximize the heat contact with air. These limitations undermine the effect of the system and prevent its further applications.[38–40]

6.1.2. Water-Based System

Water-based systems, similarly, use water as a heat transfer fluid to cool the buildings. There are two main categories, open and close systems, according to previous studies.[41,42] Open systems, exemplified by roof pond systems, are typical design with mechanical ventilation. The open water-based system runs by absorbing heat from inside and dissipating it to the surrounding heat sink by radiation and evaporation.[43] Close water-based systems, on the other hand, is consisted of pipes, where water (heat carrier flow) is inside. This kind of design has less restriction and better temperature control ability. Zhao et al.[34] developed a kW-scale radiative cooled-cold collection (RadiCold) module, which achieved a cooling effect of 10.6 °C for water at noon. By placing the system on top of buildings, a cooling power between 40 and 100 W m^{-2} was generated (Figure 8e).

The water-based system, compared to the air-based system, has a higher cooling power with better temperature control ability. However, due to the contrast between obtaining a lower outside temperature and pursuing a higher cooling performance, the technique application is also limited.[44]

6.1.3. Hybrid Systems

The air-based and water-based systems, as mentioned above, are single units of buildings cooling by radiation, which have many limits. To explore a better cooling system with a higher power, previous researchers have reported a concept of hybrid systems. As the name suggests, the hybrid system combined radiative cooling units with other energy-harvesting systems, such as radiative cooling and heat pump (RC–HP),[45] radiative

© 2020 WILEY-VCH Verlag GmbH & Co. KGaA, Weinheim

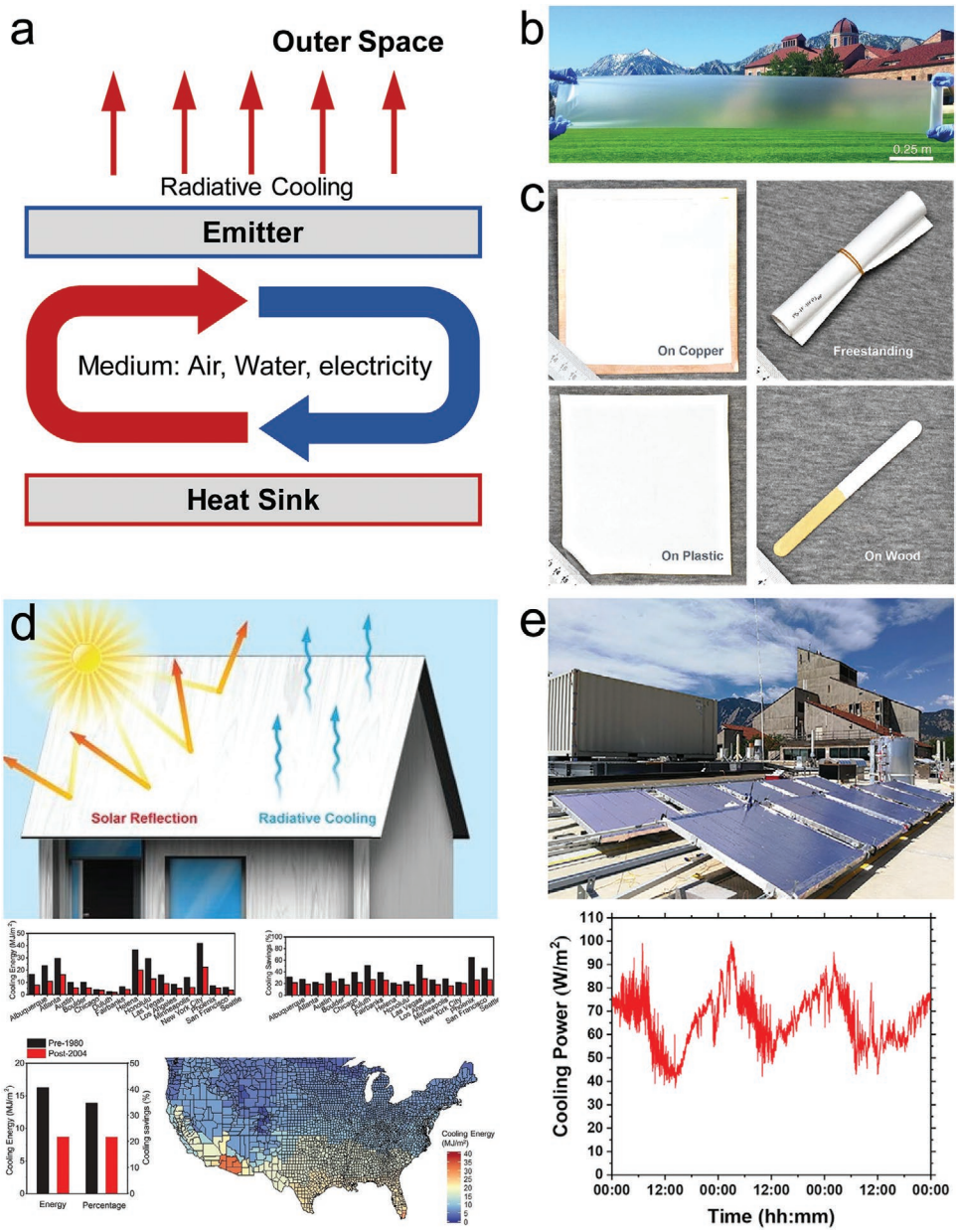

Figure 8. a) A schematic for passive radiative cooling systems in buildings. b) A photograph showing the 300 mm wide hybrid metamaterial thin film. Reproduced with permission.[2] Copyright 2017, The American Association for the Advancement of Science. c) Versatility of [P(VdF-HFP)HP] coatings. Reproduced with permission.[3] Copyright 2018, The American Association for the Advancement of Science. d) Modeling energy savings by installing cooling-wood panels on roofing and external siding of midrise apartment buildings. Reproduced with permission.[28] Copyright 2019, The American Association for the Advancement of Science. e) The kW-scale RadiCold system and its performance. Reproduced with permission.[34] Copyright 2019, Elsevier.

and evaporative cooling (RC–EC),[46–48] radiative cooling and solar energy utilization (RC–SE).[49–56] Among all, the RC–SE systems have attracted attention. Hu et al.[51] reported a system for diurnal photothermal conversion and nocturnal radiative cooling (PT–RC). Tests showed the system's thermal efficiency could reach up to 62.7%, with a net cooling power of 50.3 W m^{-2}.

Besides the photothermal conversion, integrating photovoltaic conversion with radiative cooling is also a promising method. The concept of diurnal photovoltaic and nocturnal radiative cooling hybrid system (PV–RC) was proposed by Zhao et al.[49,52] With the abilities of both harvesting electricity and cooling, the concept of PV–RC is suitable for buildings as cooling and energy harvesting systems in hot regions. Combining photovoltaic, photothermal conversion with radiative cooling, Hu et al.[57] achieved the PV–PT–RC hybrid cooling system. The PV–PT–RC system could absorb photons with energy over 1.1 eV for electricity production by silicon solar cells, while transforming the remaining photons into heat. Consequentially, the PV–PT–RC system could

© 2020 WILEY-VCH Verlag GmbH & Co. KGaA, Weinheim

obtain cooling energy and space cooling through nocturnal radiative cooling.

It is very hard to successfully apply daytime radiative cooling systems in buildings by improving individual indicators. The application of radiative cooling systems is systematic engineering: cooling effect, economic, reliability, and even aesthetics should all be considered in the process. We believe advanced radiative cooling materials and structures play particularly important roles in constructing implementable building passive cooling systems.

6.2. Personal Thermal Management

Typically, our body temperature is at a value of 37 °C, which represents the balance of heat production and heat loss in our body.[58] In order to maintain a constant and stable temperature inside the body, human thermoregulatory keeps the heat loss to the environment equal to the body's heat production.[59,60] The commonly accepted heat balance equation of the body can be described as[61]

$$M - W = E + R + C + K + S \tag{11}$$

The metabolic rate of the body (M) provides energy for the mechanical work (W) of body, and the remainder is released as heat (i.e., $M - W$). Heat realize its transfer by conduction (K), convection (C), radiation (R), and evaporation of the sweat (E). The heat storage (S) equals to the combination of heat production and loss. If a body is in heat balance, the rate of heat storage will be zero ($S = 0$). Otherwise, body temperature will keep rising or reducing. Thermal balance determines the sense of comfort in us, which can be affected by air temperature and movement, radiant temperature, relative humidity, the heat generated by human activity, and clothes.[62]

Clothing, covering the skin, has indispensable effects on body thermal comfort. It can influence the heat and moisture transfer between the body and the environment, and may protect us from the extreme hot and cold. However, in some extremely hot situations, clothing, on the other hand, can hamper the heat balance and make our body temperature keep rising.[63]

Coincidently, there is a kind of Sahara Silver Ant, which lives under the extreme hot and dry climate in the African desert, facing the same challenge. A dense array of triangular hairs composites the ant's silvery appearance, which can scatter the sunlight, as shown in **Figure 9**a. The hairs can enhance the reflectance of the silver ant's body surface within the solar spectrum range, and improve the emittance in the atmospheric transparency window. This kind of structure helps animals to dissipate heat back to the environment by radiation and maintain a heat balance under daylight conditions.[64]

Generally, in order to make ourselves comfortable in hot weather, we use the air conditioner to cool down the room. Since this method is not direct cooling, there is a lot of energy waste in this process. Moreover, we cannot make a portable air conditioner for outdoor purposes. Clothes made of radiative cooling materials can efficiently radiate heat from the body, avoid energy waste, and increase portability. Therefore, the development of personal thermal smart clothing with abilities of adjusting as circumstance change and maintaining thermal comfort is necessary.[65]

As we know, the body's thermal radiation mainly concentrates in the infrared band, so some clothes are designed to transmit the infrared radiation to the outside world to achieve cooling function. Compared with bulk ventilation and refrigeration, many more cost-effective strategies have been reported to realize personal cooling by controlling thermal radiation.[66]

Zhang et al.[68] presented a cooling textile that could change in rephrase to perspiration on human skin. By coating a thin layer of carbon nanotubes on cellulose triacetate twin crystal fibers, Zhang et al.[68] effectively modulated the infrared radiation over 35% when the relative humidity of the underlying skin changed. Due to competing hydrophobic and hydrophilic effects, bimorph fibers can be driven to change the spacing between fibers as a function of relative humidity (Figure 9c). Hsu et al.[69] designed a nanoporous polyethylene cloth, which transmitted mid-infrared human radiation but not visible light. They further developed the fabric that improved radiative cooling performance while still having sufficient breathability, water absorption, and mechanical strength to improve wear resistance (Figure 9d). Tong et al.[71] proposed an infrared transparent visible-opaque fabric (ITVOF) model for personal thermal management radiative cooling system. They used ITVOF to develop a new method of personal cooling, a technology that radiates heat from human bodies directly to the surrounding environment. The fiber is structurally designed to minimize IR reflections through weak Rayleigh scattering while maintaining a high opacity with strong Mie scattering.

Hsu et al.[70] reported a personal thermal management system using fabrics with embedded metal nanowires. Metal nanowires not only had high thermal insulation properties, but also formed a conductive network that could supplement passive insulation layers with Joule heating. Due to the porous structure of the nanowires, the breathability and durability of the original fabric were still maintained (Figure 9e). Cai et al.[67] designed a novel textile of polyethylene embedded ZnO nanoparticles, which had a spectral selectivity. This textile could reflect over 90% of solar spectrum and radiate human body heat selectively. Tests showed this textile could cool the simulated skin by 5–13 °C (Figure 9b). In addition, Cai et al.[73] presented a new type of textile based on nanoporous metallized polyethylene, which was designed to meet the needs of passive heating spectral selection. By putting an IR reflective layer on an IR transparent layer embedded with nanopores, the textile achieved a minimum IR emissivity of about 10% on its outer surface, thereby effectively reducing the thermal radiation loss. The design reduced skin temperature by 7 °C compared to normal textiles without sacrificing wearing comfort.

Hsu et al.[72] demonstrated a dual-mode textile that could reach both passive radiative cooling and heat without input energy, which increased the thermal comfort zone by 6.5 °C. By embedding a bilayer emitter inside an infrared-transparent nanoporous polyethylene (nanoPE) layer, the textile could heat up when the low emissivity layer faces outward, and cool down when high emissivity layer faces outward. Peng et al.[74] reported a large-extrusion method of manufacturing uniform and continuous nanoporous polyethylene (nanoPE) microfibers. Textiles made of nanoPE microfibers not only had impressive wear resistance

© 2020 WILEY-VCH Verlag GmbH & Co. KGaA, Weinheim

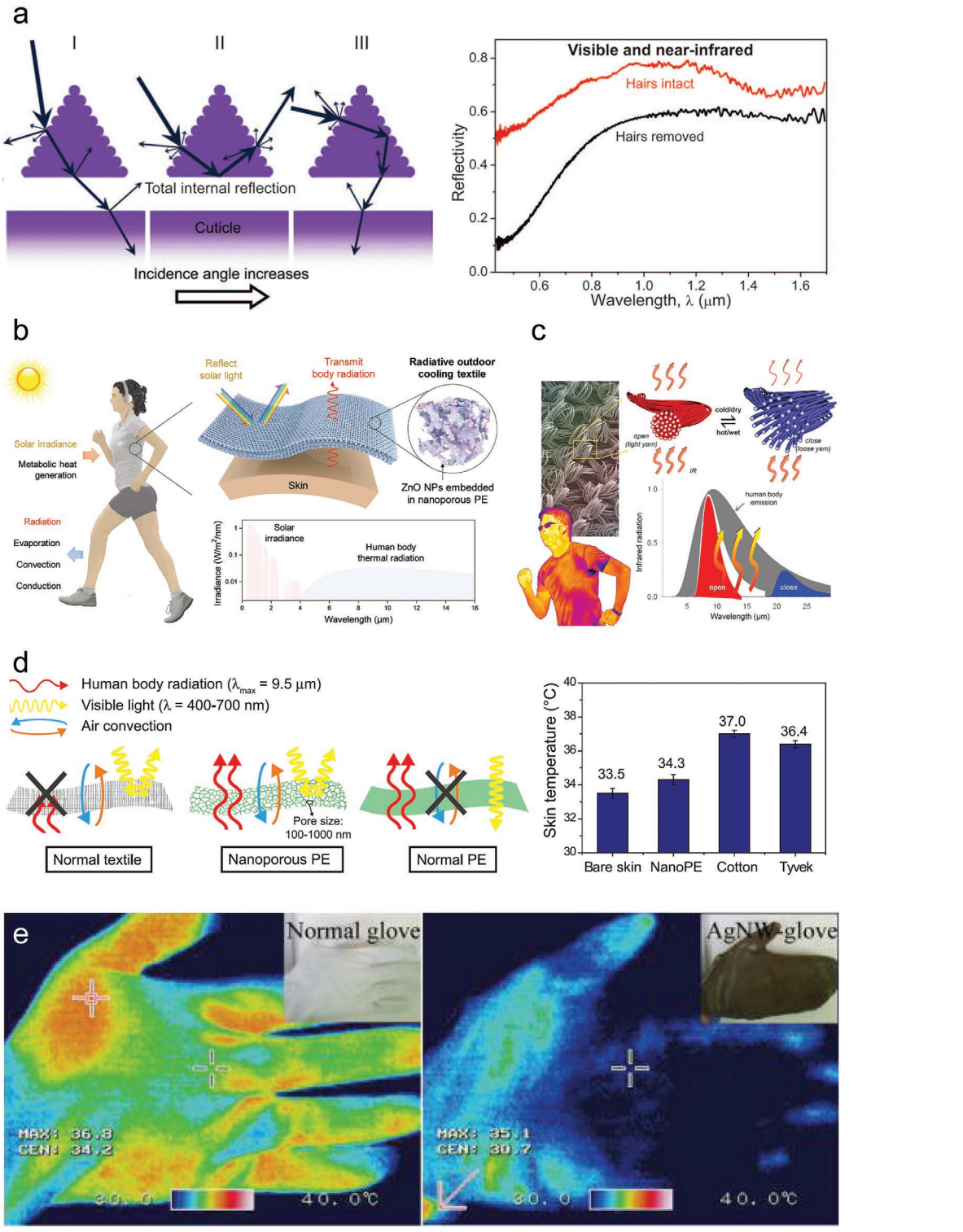

Figure 9. a) Left: Schematic diagram showing the interaction between visible and NIR light and hair. Right: Hemispherical reflectivity measured in the visible and NIR. Reproduced with permission.[64] Copyright 2015, The American Association for the Advancement of Science. b) Schematic illustrating the heat input and output pathways of the human body under sunlight in the outdoor environment, schematic of the ZnO nanoparticle-embedded nanoporous polyethylene (nanoPE) textile and Spectrum comparison of AM 1.5 Global solar irradiation and human body thermal radiation. Reproduced with permission.[67] Copyright 2018, John Wiley and Sons. c) Design principles of an IR gating textile. Reproduced with permission.[68] Copyright 2019, The American Association for the Advancement of Science. d) Schematics of comparison between nanoPE, normal PE, and cotton and Thermal measurement. Reproduced with permission.[69] Copyright 2016, The American Association for the Advancement of Science. e) Side-by-side comparison of thermal images of a human hand with a normal glove and with an AgNW glove, proving the scalability and effectiveness of the dip-coated AgNW cloth. Reproduced with permission.[70] Copyright 2015, American Chemical Society.

© 2020 WILEY-VCH Verlag GmbH & Co. KGaA, Weinheim

and durability compared with commercial cotton fabrics, but also possessed excellent cooling performance. Tests showed the nanoPE fabrics could cool human skin by 2.3 °C, which is equivalent to saving indoor cooling energy by more than 20%.

The colors and styles also play an indispensable role in clothing. Daytime radiative cooling textiles, due to the demanding of high-reflection in the visible light band, always present white. Cai et al.[75] reported a new strategy for using inorganic nanoparticles as a coloring component in a scalable, bright-colored infrared transparent textile. The composite fabric had a high infrared transmission of about 80% and an outstanding cooling capacity of 1.6–1.8 °C. At the same time, these textiles showed a strong visible color and excellent washing stability.

6.3. Adjustable Radiative Cooling

Usually, the existing radiative cooling technologies are static structures. However, with phase-change materials (PCM), researchers were able to develop dynamic structures corresponding to weather variations. Wu et al.[76] presented a design of VO_2-coated microcones that had the ability of switchable thermal emission. The thin film VO_2 on silicon microcones, a common temperature-induced PCM, controlled the intensity of emissivity. When the temperature was below the phase transfer temperature, the structure had a low emissivity (insulating state of VO_2); otherwise, the emissivity was high (metallic state of VO_2). Similarly, Wu et al.[77] reported a multilayer structure of $VO_2/SiO_2/VO_2$ that could achieve switchable temperature control. The meta-surface had a theoretically fourfold tunable radiative cooling power density, when the device temperature changed below/above the VO_2's phase change temperature. Kort-Kamp et al.[78] and Ono et al.[79] also proposed similar PCM-based structures.

Besides PCM-based structures, water can also contribute to the switchability of radiative structures. Mandal et al.[80] showed that porous polymer coatings (PPC), of which the transmittance to solar and infrared radiation changes upon wetting, could be used for seasonal thermal regulation. For polyethylene PCC, wetting leads to a transition from radiative cooling to radiative heating. The dynamic feature of PCC-based devices is attractive in radiative cooling applications.

By taking advantage of switchable materials and structures, radiative cooling systems have the ability of thermal regulation corresponding to the environmental changes.

7. Conclusion and Outlook

In this paper, we reviewed the fundamental principles for radiative cooling, approaches to achieve nocturnal and diurnal cooling effects, and various applications in buildings, air conditioning, water cooling, and clothing. We anticipate that radiative cooling can realize remarkable cooling performance and have a promising future of thermal management. However, there are also a few issues and limitations that need to be considered before it can make a real impact. For example, the radiative cooling performance is strongly dependent upon weather conditions, and therefore cannot serve as a stable source of cooling power. Here, we would also like to discuss some possible pathways for further studies.

First, though recent researches have already realized considerable net cooling power, it is not easy to harness the energy in the form of radiative cooling. This form of energy is not as versatile as electricity or cold water, and thus a transformation is desirable. Moreover, as we know, instead of inside the bulk, radiative cooling only happens on the materials' upper surfaces. To achieve a cooling effect, take the case of the rooftop cooler, the heat of the building must pass through the devices from the backside to the surface, and a low-thermal-conduction medium will excessively block the heat transfer process. Therefore, it is of both mechanical and thermal challenges to build such a system that has a high energy utilization rate. At the present stage, air-based and water-based devices are two kinds of systems that can convert the surface cooling energy into more easy-to-use energy forms.

The hybrid system, on the other hand, has not been thoroughly investigated. As shown in **Figure 10**b, two viable theoretical models were proposed by Byrnes et al.[82] This work shows the possibility of changing the cooling power into electricity and other energy forms through a heat engine or diode-resistor circuits. Later, as reported by Raman et al.,[81] other than using air or water as conversion media, we can couple the cooling panels with thermoelectric systems and transfer the cooling energy into electricity (Figure 10a). A hybrid system with this design could generate a power of 25 mW m^{-2} and light an LED at night. Besides, note that many cooling films are transparent, by stacking the radiative cooling devices on other cooling systems, the cooling power can further improve. There are significant opportunities for some hybrid systems to overcome the challenge and accomplish effective energy conversion.

Second, due to the weather changes, the cooling performance varies all the time. Coupling the cooling devices with heat storage can help provide stable power output. Alternatively, we can take advantage of the changes, i.e., by combining photothermal conversion and radiative heating with radiative cooling, a tunable, comprehensive, weatherproof, all-time power source can be obtained.

Third, as to radiative cooling clothing, improvement can be made from a number of different dimensions, either functional or aesthetic. Eligible clothes should satisfy many requirements simultaneously, including wearability, air permeability, washing stability, and durability. Color is also a desirable feature for clothing because of aesthetic appeals. In spite of most of the radiative cooling materials being transparent or white, novel designs provided by Cai et al.[75] modulated the visible spectrum of the cooling materials and exhibited intense colors (Figure 10c). Though the colored textiles were cooler than cotton, the temperature was still higher than bare skin. Narrowband, pinpoint control over visible spectrum is needed for promoting temperature reduction and for offering ample choices of color. We suggest all these factors be taken into account comprehensively in designing for commercial clothing or textiles.

Finally, colored cooling materials can also be employed in many outdoor scenarios. As indicated in a recent-reported colored photonic crystal material design,[83] there are significant opportunities for rooftop applications. Without changing the

© 2020 WILEY-VCH Verlag GmbH & Co. KGaA, Weinheim

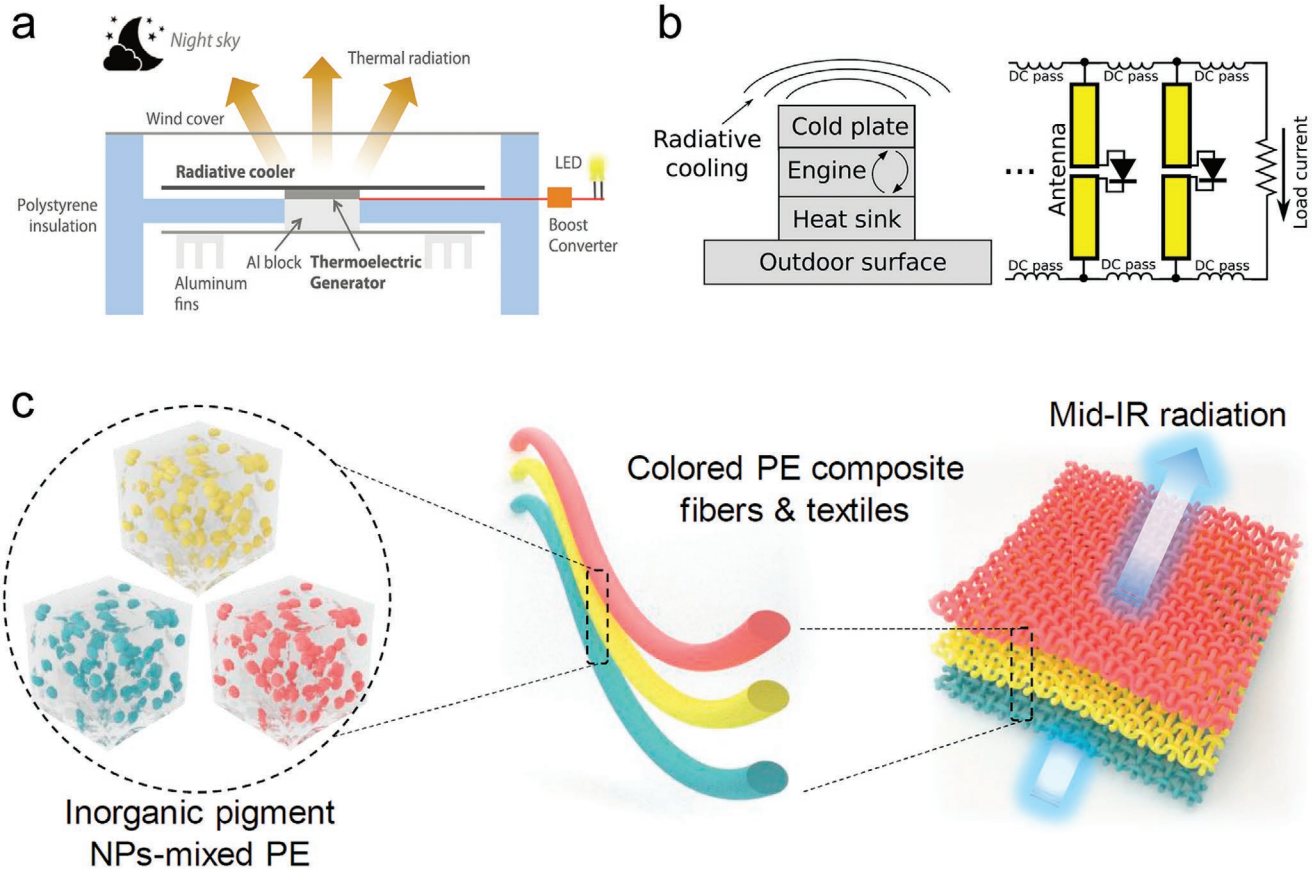

Figure 10. a) Schematic of the low-cost night-time thermoelectric generator device and its key components. Reproduced with permission.[81] Copyright 2019, Elsevier. b) Two possible emissive energy harvester (EEH) designs. Left: In a thermal EEH, a heat engine operates between the ambient temperature and a radiatively cooled plate. Right: In an infrared rectenna EEH, the whole panel is at ambient temperature, but the circuit's electrical noise is coupled to the cold radiation field via antennas. Reproduced with permission.[82] Copyright 2014, National Academy of Sciences. c) Design schematic for the coloration of radiative cooling textiles, which is made by mixing IR transparent inorganic pigment nanoparticles with polyethylene (PE). Reproduced with permission.[75] Copyright 2019, Elsevier.

visual perception, we can expect the colored radiative cooling materials to tailor the thermal load for buildings and other outdoor environments.

Acknowledgements

This article is part of the Advanced Materials Technologies Hall of Fame article series, which recognizes the excellent contributions of leading researchers to the field of technology-related materials science. Z.L. and Q.C. contributed equally to this work. The authors acknowledge the microfabrication center of the National Laboratory of Solid State Microstructures (NLSSM) for technical support. This work was jointly supported by the National Key Research and Development Program of China (Grant No. 2017YFA0205700), the National Natural Science Foundation of China (Grant Nos. 11874211, 11574143, 21805132, 11621091, and 61735008), the Natural Science Foundation of Jiangsu Province (Grant No. BK20180341), and the Fundamental Research Funds for the Central Universities (Grant Nos. 021314380140 and 021314380150).

Conflict of Interest

The authors declare no conflict of interest.

Keywords

atmospheric transparency window, building cooling, daytime radiative cooling, personal thermal management, selective emitters

Received: November 11, 2019
Revised: December 20, 2019
Published online:

[1] A. P. Raman, M. A. Anoma, L. Zhu, E. Rephael, S. Fan, *Nature* **2014**, *515*, 540.
[2] Y. Zhai, Y. Ma, S. N. David, D. Zhao, R. Lou, G. Tan, R. Yang, X. Yin, *Science* **2017**, *355*, 6329.
[3] J. Mandal, Y. Fu, A. C. Overvig, M. Jia, K. Sun, N. N. Shi, H. Zhou, X. Xiao, N. Yu, Y. Yang, *Science* **2018**, *362*, 6412.
[4] C. G. Granqvist, A. Hjortsberg, *J. Appl. Phys.* **1981**, *52*, 4205.
[5] G Observatory, http://www.gemini.edu/sciops/telescopes-and-sites/observing-condition-constraints/ir-transmission-spectra (accessed: September 2019).
[6] B. Bhatia, A. Leroy, Y. Shen, L. Zhao, M. Gianello, D. Li, T. Gu, J. Hu, M. Soljačić, E. N. Wang, *Nat. Commun.* **2018**, *9*, 5001.
[7] S. Catalanotti, V. Cuomo, G. Piro, D. Ruggi, G. Troise, *Sol. Energy* **1975**, *17*, 83.
[8] E. Rephaeli, A. Raman, S. Fan, *Nano Lett.* **2013**, *13*, 1457.

© 2020 WILEY-VCH Verlag GmbH & Co. KGaA, Weinheim

[9] A. K. Head, *US3043112A*, **1962**.
[10] E. M. Lushiku, A. Hjortsberg, C. G. Granqvist, *J. Appl. Phys.* **1982**, *53*, 5526.
[11] F. Trombe, *Rev. Gen. Therm.* **1967**, *6*, 1285.
[12] Ph. Grenier, *Rev. Phys. Appl.* **1979**, *14*, 87.
[13] T. M. J. Nilsson, G. A. Niklasson, *Sol. Energy Mater. Sol. Cells* **1995**, *37*, 93.
[14] B. Bartoli, S. Catalanotti, B. Coluzzi, V. Cuomo, V. Silvestrini, G. Troise, *Appl. Energy* **1977**, *3*, 267.
[15] C. G. Granqvist, A. Hjortsberg, T. S. Eriksson, *Thin Solid Films* **1982**, *90*, 187.
[16] T. S. Eriksson, C. G. Granqvist, *Appl. Opt.* **1983**, *22*, 3204.
[17] T. S. Eriksson, S. J. Jiang, C. G. Granqvist, *Sol. Energy Mater.* **1985**, *12*, 319.
[18] A. R. Gentle, G. B. Smith, *Nano Lett.* **2010**, *10*, 373.
[19] P. Berdahl, *Appl. Opt.* **1984**, *23*, 370.
[20] A. W. Harrison, M. R. Walton, *Sol. Energy* **1978**, *20*, 185.
[21] B. Orel, M. K. Gunde, A. Krainer, *Sol. Energy* **1993**, *50*, 477.
[22] A. Addeo, L. Nicolais, G. Romeo, B. Bartoli, B. Coluzzi, V. Silvestrini, *Sol. Energy* **1980**, *24*, 93.
[23] A. R. Gentle, G. B. Smith, *Adv. Sci.* **2015**, *2*, 1500119.
[24] Z. Chen, L. Zhu, A. Raman, S. Fan, *Nat. Commun.* **2016**, *7*, 13729.
[25] M. M. Hossain, B. Jia, M. Gu, *Adv. Opt. Mater.* **2015**, *3*, 1047.
[26] L. Zhu, A. P. Raman, S. Fan, *Proc. Natl. Acad. Sci. USA* **2015**, *112*, 12282.
[27] S. H. Wu, M. Chen, M. T. Barako, V. Jankovic, P. W. C. Hon, L. A. Sweatlock, M. L. Povinelli, *Optica* **2017**, *4*, 1390.
[28] T. Li, Y. Zhai, S. He, W. Gan, Z. Wei, M. Heidarinejad, D. Dalgo, R. Mi, X. Zhao, J. Song, J. Dai, C. Chen, A. Aili, A. Vellore, A. Martini, R. Yang, J. Srebric, X. Yin, L. Hu, *Science* **2019**, *364*, 6442.
[29] C. Liu, Y. Wu, B. Wang, C. Y. Zhao, H. Bao, *Sol. Energy* **2019**, *183*, 218.
[30] A. Leroy, B. Bhatia, C. C. Kelsall, A. Castillejo-Cuberos, M. Di Capua H., L. Zhao, L. Zhang, A. M. Guzman, E. N. Wang, *Sci. Adv.* **2019**, *10*, 9480.
[31] MODTRAN, https://modtran.spectral.com/modtran_home#plot (accessed: September 2019).
[32] C. Y. Tso, K. C. Chan, C. Y. H. Chao, *Renewable Energy* **2017**, *106*, 52.
[33] A. M. Omer, *Renewable Sustainable Energy Rev.* **2008**, *12*, 2265.
[34] D. Zhao, A. Aili, Y. Zhai, J. Lu, D. Kidd, G. Tan, X. Yin, R. Yang, *Joule* **2019**, *3*, 111.
[35] X. Lu, P. Xu, H. Wang, T. Yang, J. Hou, *Renewable Sustainable Energy Rev.* **2016**, *65*, 1079.
[36] K. N. Nwaigwe, C. A. Okoronkwo, N. V. Ogueke, *Int. J. Energy. Clean Environ.* **2010**, *11*, 117.
[37] B. Givoni, *Energy Build.* **1977**, *1*, 141.
[38] G. Mihalakakou, A. Ferrante, J. O. Lewis, *Energy Build.* **1998**, *28*, 251.
[39] H. S. Bagiorgas, G. Mihalakakou, *Renewable Energy* **2008**, *33*, 1220.
[40] J. Khedari, J. Waewsak, S. Thepa, J. Hirunlabh, *Renewable Energy* **2000**, *20*, 183.
[41] S. N. Kharrufa, A. Yahyah, *Build. Environ.* **2008**, *43*, 82.
[42] M. S. Sodha, U. Singh, A. Srivastava, G. N. Tiwari, *Build. Environ.* **1981**, *16*, 93.
[43] N. M, Nahar, P. S, M. M. Purohit, *Build. Environ.* **2003**, *38*, 109.
[44] A. H. H. Ali, *Energy Convers. Manage.* **2007**, *48*, 93.
[45] Y. Man, H. Yang, J. D. Spitler, Z. Fang, *Appl. Energy* **2011**, *88*, 4160.
[46] F. M. Farahani, G. Heidarinejad, S. Delfani, *Energy Build.* **2010**, *42*, 2131.
[47] F. M. Farahani, G. Heidarinejad, *Appl. Therm. Eng.* **2012**, *38*, 117.
[48] G. Heidarinejad, F. M. Farahani, S. Delfani, *Build. Environ.* **2010**, *45*, 1521.
[49] B. Zhao, M. Hu, X. Ao, G. Pei, *Appl. Energy* **2017**, *205*, 626.
[50] M. Hu, B. Zhao, J. Li, Y. Wang, G. Pei, *Energy* **2017**, *137*, 419.
[51] M. Hu, G. Pei, Q. Wang, J. Li, Y. Wang, J. Ji, *Appl. Energy* **2016**, *179*, 899.
[52] B. Zhao, M. Hu, X. Ao, Q. Xuan, G. Pei, *Sol. Energy Mater. Sol. Cells* **2018**, *178*, 266.
[53] M. Hu, B. Zhao, X. Ao, Y. Su, Y. Wang, G. Pei, *Energy* **2018**, *155*, 360.
[54] U. Eicker, A. Dalibard, *Sol. Energy* **2011**, *85*, 1322.
[55] M. Hu, G. Pei, L. Li, R. Zheng, J. Li, J. Ji, *Int. J. Photoenergy* **2015**, *2015*, 807875.
[56] M. Fiorentini, P. Cooper, Z. Ma, *Energy Build.* **2015**, *94*, 21.
[57] M. Hu, B. Zhao, X. Ao, P. Zhao, Y. Su, G. Pei, *Appl. Energy* **2018**, *231*, 288.
[58] G. Havenith, *Ann. Occup. Hyg.* **1999**, *43*, 289.
[59] P. O. Fanger, *Br. J. Ind. Med.* **1973**, *30*, 313.
[60] H. R. Mattila, *Intelligent Textiles and Clothing*, Woodhead/The Textile Institute, Cambridge **2006**.
[61] K. C. Parsons, *Human Thermal Environments*, 3rd ed., CRC Press, London **2013**.
[62] N. Djongyang, R. Tchinda, D. Njomo, *Renewable Sustainable Energy Rev.* **2010**, *14*, 2626.
[63] G. Havenith, *Exog. Dermatol.* **2002**, *1*, 221.
[64] N. N. Shi, C. C. Tsai, F. Camino, G. D. Bernard, N. Yu, R. Wehner, *Science* **2015**, *349*, 6245.
[65] K. Choi, G. Cho, P. Kim, C. Cho, *Text. Res. J.* **2004**, *74*, 292.
[66] J. M. Stapleton, C. Q. Lan, S. G. Hardcastle, presented at Proc. 13th Int. Conf. on Environmental Ergonomics, Boston, MA, August **2014**.
[67] L. Cai, A. Y. Song, W. Li, P. C. Hsu, D. Lin, P. B. Catrysse, Y. Liu, Y. Peng, J. Chen, H. Wang, J. Xu, A. Yang, S. Fan, Y. Cui, *Adv. Mater.* **2018**, *30*, 1802152.
[68] X. A. Zhang, S. Yu, B. Xu, M. Li, Z. Peng, Y. Wang, *Science* **2019**, *363*, 619.
[69] P. Hsu, A. Y. Song, P. B. Catrysse, C. Liu, Y. Peng, J. Xie, S. Fan, Y. Cui, *Science* **2016**, *353*, 1019.
[70] P. Hsu, X. Liu, C. Liu, X. Xie, H. R. Lee, A. J. Welch, T. Zhao, Y. Cui, *Nano Lett.* **2015**, *15*, 365.
[71] J. K. Tong, X. Huang, S. V. Boriskina, J. Loomis, Y. Xu, G. Chen, *ACS Photonics* **2015**, *2*, 769.
[72] P. Hsu, C. Liu, A. Y. Song, Z. Zhang, Y. Peng, J. Xie, K. Liu, C. Wu, P. B. Catrysse, L. Cai, S. Zhai, A. Majumdar, S. Fan, Y. Cui, *Sci. Adv.* **2017**, *3*, e1700895.
[73] L. Cai, A. Y. Song, P. Wu, P. C. Hsu, Y. Peng, J. Chen, C. Liu, P. B. Catrysse, Y. Liu, A. Yang, C. Zhou, C. Zhou, S. Fan, Y. Cui, *Nat. Commun.* **2017**, *8*, 496.
[74] Y. Peng, J. Chen, A. Y. Song, P. B. Catrysse, P. C. Hsu, *Nat. Sustain.* **2018**, *1*, 105.
[75] L. Cai, Y. Peng, J. Xu, C. Zhou, C. Zhou, P. Wu, D. Lin, *Joule* **2019**, *3*, 1478.
[76] S. H. Wu, M. Chen, M. T. Barako, V. Jankovic, P. W. C. Hon, *Optica* **2017**, *4*, 1390.
[77] S. Wu, K. Lai, C. Wang, *Sci. Rep.* **2018**, *8*, 7684.
[78] W. J. M. Kort-Kamp, S. Kramadhati, A. K. Azad, M. T. Reiten, D. A. R. Dalvit, *ACS Photonics* **2018**, *5*, 4554.
[79] M. Ono, K. Chen, W. Li, S. Fan, *Opt. Express* **2018**, *26*, A777.
[80] J. Mandal, M. Jia, A. Overvig, Y. Fu, E. Che, N. Yu, Y. Yang, *Joule* **2019**, *3*, 3088.
[81] A. P. Raman, W. Li, S. Fan, *Joule* **2019**, *3*, 2679.
[82] S. J. Byrnes, R. Blanchard, F. Capasso, *Proc. Natl. Acad. Sci. USA* **2014**, *111*, 3927.
[83] W. Li, Y. Shi, Z. Chen, S. Fan, *Nat. Commun.* **2018**, *9*, 4240.
[84] B. Zhao, M. Hu, X. Ao, N. Chen, G. Pei, *Appl. Energy* **2019**, *236*, 489.

© 2020 WILEY-VCH Verlag GmbH & Co. KGaA, Weinheim